EFFECTS OF VEGETATION ON BEYOND 4G COMMUNICATIONS

by

POH SOON CHANG

1122702429

Session 2016/2017

The project report is prepared for
Faculty of Engineering
Multimedia University
in partial fulfilment for
Bachelor of Engineering (Hons) Electronics

FACULTY OF ENGINEERING
MULTIMEDIA UNIVERSITY

February 2017

DECLARATION

I hereby declare that this work has been done by myself and no portion of the work contained in this report has been submitted in support of any application for any other degree or qualification of this or any other university or institute of learning.

I also declare that pursuant to the provisions of the Copyright Act 1987, I have not engaged in any unauthorised act of copying or reproducing or attempt to copy / reproduce or cause to copy / reproduce or permit the copying / reproducing or the sharing and / or downloading of any copyrighted material or an attempt to do so whether by use of the University's facilities or outside networks / facilities whether in hard copy or soft copy format, of any material protected under the provisions of sections 3 and 7 of the Act whether for payment or otherwise save as specifically provided for therein. This shall include but not be limited to any lecture notes, course packs, thesis, text books, exam questions, any works of authorship fixed in any tangible medium of expression whether provided by the University or otherwise.

I hereby further declare that in the event of any infringement of the provisions of the Act whether knowingly or unknowingly the University shall not be liable for the same in any manner whatsoever and undertakes to indemnify and keep indemnified the University against all such claims and actions.

Signature: _____

Name: Poh Soon Chang

Student ID: 1122702429

Date:

ACKNOWLEDGEMENT

I would like to express my most sincere gratitude to all who provided all their support, guidance and help to me when I was doing this project. Without them, the process of doing this project and completing the thesis would not be as exciting and meaningful as it was.

Firstly, I would like thank Miss Siva Priya Thiagarajah for the opportunity of doing this project under her guidance throughout the past two trimesters. Throughout this period, she provided me with brilliant suggestions and motivations that help me to complete this project. Further, I would like to thank my peers, Ho Chit On and Tan Guo Zheng for their invaluable comments on my project.

I am thankful for my family for their love and moral support. Without them, completion of project would not be as meaningful as it was. I would like to thank my friends for sharing their ideas with me.

ABSTRACT

5G systems require frequency bands from millimetre wave spectrum with big and contiguous bandwidth to satisfy expected demand of higher capacity in the future. This project aims to study the effects of vegetation on millimetre wave propagation. In addition, the effects of tree species common in an urban propagation environment such as Kuala Lumpur, Malaysia on millimetre wave propagation were investigated.

First of all, a suitable model was selected out of a number of existing models which were designed for predicting effects of vegetation on signal propagation. The models can be grouped as empirical model or analytical model. The review of the models was based on literature review and reinforced with verification through software simulation of the models. Out of all the models, RET model based on Radiative Energy Transfer (RET) was selected because it takes into account background physical processes such as scattering and absorption by the vegetation body. Eventually, an ITU-R model which includes the selected RET model as through vegetation component was implemented using MATLAB for this project at 37 GHz. The ITU-R model takes into account additional physical processes such as ground reflection and diffraction. In addition, the RET model or through vegetation component of the ITU-R model was enhanced to approximates hemispherical and spherical crown shapes of tree species common for tree planting in Kuala Lumpur, Malaysia to study their effects on millimetre wave propagation.

The findings of the project are based on MATLAB simulation results. It was found that through vegetation attenuation is higher for a signal of higher frequency. The plot of through vegetation attenuation against vegetation depth has dual slope characteristic. For a D2D connection under the tree, the ground reflection loss is in order of tens of dB for grazing angle around 45 º at 37 GHz. As for diffractions, the diffraction loss is in order of hundreds of dB. Last but not least, it is concluded that the enhanced through vegetation component or RET model provides more realistic predictions by 7.59% and 3.83% for hemispherical and spherical crown respectively. The findings are intuitive and useful for future 5G deployment if it uses 37 GHz to 40.5 GHz as its frequency band.

TABLE OF CONTENTS

LIST OF FIGURES

LIST OF TABLES

LIST OF ABBREVIATIONS

LTE	Long Term Evolution
4G	Fourth generation wireless mobile telecommunications technology
5G	Fifth generation wireless mobile telecommunications technology
MHz	Megahertz
GHz	Gigahertz
mm-wave	Millimetre wave
ITU	International Telecommunication Union
ITU-R	International Telecommunication Union Recommendation
MCMC	Malaysian Communications and Multimedia Commission
WRC	World Radiocommunication Conference
dB	Decibel
m	Meters

CHAPTER 1 INTRODUCTION

1.1 Overview

It was predicted that incremental upgrades to existing 4G mobile wireless communication technology such as LTE Advanced Pro would be unable to satisfy market's demand for higher capacity by 2020 [1]. Therefore, development of a new communication technology which has capabilities far beyond current 4G technology is necessary. This next generation of mobile wireless communication technology is more commonly known as "5G". 5G is expected to have high peak data rate of several gigabits-per-second [2]. Shannon's formula states that, the capacity of a channel is directly proportional to its bandwidth. Therefore, future 5G frequency bands require bandwidth ranging from several hundred MHz to 1 GHz [2]. Currently, there are a number of frequency bands from the mm-wave spectrum (30 to 300 GHz) that fulfils the requirement of having aforementioned large bandwidth [3]. Waves of these bands have propagation characteristics which are different than those of 4G bands. There are many investigations that were carried out to study the propagation characteristics of waves from mm-wave spectrum. One of the focuses of these studies is propagation characteristics of mm-wave in a vegetative medium.

1.2 Objectives

The objectives of this project are:

1. To study and analyze the effects of vegetation on mm-wave propagation using a suitable prediction model.
2. To investigate the effects of urban tree species in Kuala Lumpur, Malaysia on mm-wave propagation.

1.3 Problem Statement

A number of frequency bands from near mm-wave spectrum and mm-wave spectrum were selected as 5G candidate bands [4]. Waves of these bands have wavelengths in order of millimetres which are comparable to leaves and branches of certain species of trees. As a result, propagation characteristics of these waves are different from

waves of 4G bands. Therefore, knowledge from past 4G researches may be inapplicable. In addition, according to statement presented in the paper by Rappaport et al., there is relatively little knowledge of mm-wave propagation [3]. With reference to this statement, signal propagation in a vegetative medium at frequencies of mm-wave spectrum has been identified as the problem that requires investigation as it is important for future development and deployment of 5G.

1.4 Project Scope

The scope of this project is the study of mm-wave propagation characteristics in an environment with presence of vegetation. The study is based on results of software simulation of an existing model which is best suited for predicting mm-wave propagation in a vegetative medium. There are a number of models available. They can be broadly categorized into empirical model and analytical model. These models will be reviewed and verified based on software simulation and literature review. Furthermore, the selected model is enhanced to study the effects of urban tree species in Kuala Lumpur, Malaysia on mm-wave propagation.

1.4 Report Outline

This thesis presents an overview of future mobile communications and an introduction into the focus of this project in Chapter 1. Reviews of literature such as journal papers were summarized and presented in Chapter 2. In addition, Chapter 2 contains the descriptions and software simulations for certain models that were reviewed. Chapter 3 describes the implementation of the project in details. It includes descriptions of an analytical model which was recommended by ITU-R and some enhancement to it. Next, Chapter 4 presents the findings of the project. It also consists of discussions on the results. This report ends with Chapter 5 which consists of summary and conclusion.

CHAPTER 2 LITERATURE REVIEW

2.1 Introduction

This chapter is about the literature review that was conducted. Section 2.2 is about 5G candidate bands. Section 2.3 describes vegetation attenuation. There are two general groups of models, empirical model and analytical model. Section 2.4 is all about empirical model. The empirical models can be further grouped as Modified Exponential Decay (MED) model and Modified Gradient model. They are explained in Section 2.4.1 and 2.4.2 respectively. There are 3 MED models, which are Weissberger model, Fitted ITU-R model and COST 235 model. They are presented from Section 2.4.1.1 till 2.4.1.3. Section 2.4.1.4 includes software simulations of MED models. Section 2.4.2.1 and 2.4.2.2 and 2.4.2.3 are about Maximum Attenuation model, Nonzero Gradient model and Dual Gradient model respectively. Section 2.5 is about the only analytical model based on Radiative Energy Transfer (RET) theory. Section 2.6 contains a summary of all the reviewed models and the details of selection of model to be used for this project. Section 2.7 describes device-to-device (D2D) connections.

2.2 5G Candidate Bands

One of the requirements of 5G is high data rate of several gigabits-per-second [2]. According to Shannon's capacity formula, a channel with higher capacity has a larger bandwidth. To achieve intended high capacity, 5G candidate bands must have large bandwidth, ranging from 500 MHz to several GHz [5]. Therefore, researchers laid their eyes on several bands from mm-wave spectrum (30 GHz to 300 GHz) because these bands are contiguous and have large bandwidth [3]. On the other hand, mobile service operators were attracted by these bands because they are relatively unused and lightly licensed [6].

The world is divided into 3 regions by ITU with varying frequency band allocations. Malaysia is located in Region 3 [7]. During WRC 2015 at Geneva, several frequency bands from near mm-wave spectrum and mm-wave spectrum were selected by ITU-R for sharing and compatibility study in time for WRC 2019 [4]. According to

spectrum plan released by MCMC [8], these frequency bands are primarily allocated for mobile services. Besides from allocation for mobile services, some of these bands are also allocated for other services. Table 2.1 shows a quick high level investigation of co-existence with satellite services for the selected bands based on MCMC's spectrum plan document. Sharing study based on only MCMC's spectrum plan is not practical since Malaysia is only one voice in the region. It is hard to tell which of these bands will be the 5G band in the future since sharing and compatibility study is no easy task and out of the scope of this project. Co-existence of services may interfere with future 5G mobile services. It is important to develop innovative sharing methods and minimizing co-existences in addition to developing higher performance 5G systems to overcome sharing issues [9].

Table 2.1 ITU-R's selected bands

Bands (GHz)	Satellite services presence (Yes / No)
24.25-27.5	Yes
37-40.5	Yes
42.5-43.5	Yes
45.5-47	-
47.2-50.2	Yes
50.4-52.6	Yes
66-76	Yes
81-86	Yes

Beside from ITU-R's bands, the frequency band of 27.5 GHz to 29.5 GHz or more commonly known as the 28 GHz band is another popular 5G candidate band which was extensively studied and researched in United States of America and South Korea [6]. In Malaysia, this band has primary allocation for mobile services.

2.3 Vegetation attenuation

Vegetation attenuation is signal loss when the line of sight path between transmitter and receiver is blocked by a vegetative medium. For mobile communications, the blocking vegetative medium can either be a single tree or line of trees as shown in Figure 2.1 [10].

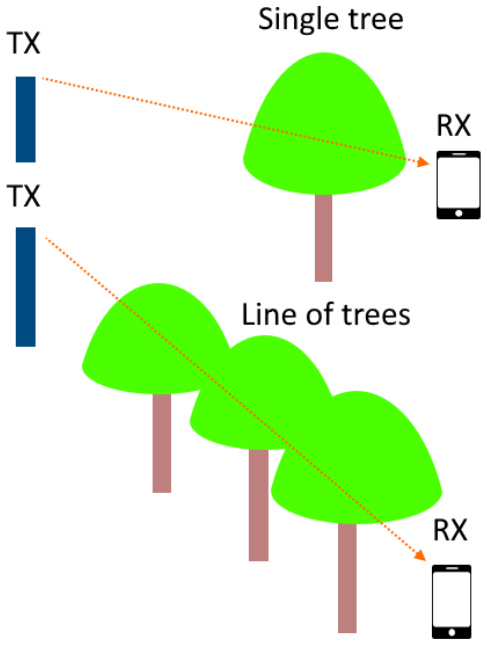

Figure 2.1: Single tree and line of trees as blocking medium

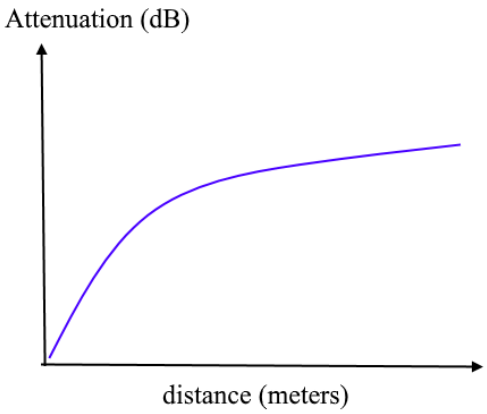

Figure 2.2: Dual slope characteristics of curve of attenuation (dB) against distance (meters)

As shown in Figure 2.2, the curve of measured attenuation (dB) against vegetation depth (meters) has two slopes [11]. This characteristic is known as dual slope characteristic [12]. Based on Figure 2.2, this curve has a steeper initial slope followed by a less steep slope. According to Radiative Energy Transfer (RET) theory, the higher initial attenuation rate is due to loss experienced by the coherent component of the signal [13]. At a longer depth, the incoherent component overtakes the coherent component with a lower attenuation rate or a less steep slope [13]. The details about coherent component and incoherent component are presented in Section 2.5.

2.4 Empirical Model

Empirical path loss model is formulated from measurement data which were obtained from extensive measurement activities [10]. They are designed to give best fits to measurement data [14]. Their benefits lie in their simplicity [10].

There are two general categories of empirical model for predicting vegetation attenuation. They are Modified Exponential Decay (MED) model [10] and Modified Gradient model [10].

2.4.1 Modified Exponential Decay Model

The Modified Exponential Decay (MED) model has the following general formula given by [10]:

$$L\ (dB) = X \times f^{Y} d^{Z} \tag{2.1}$$

where f is frequency, d is depth into vegetation in meters, X, Y, Z are fitted parameters from measurement data.

The values of X, Y and Z are formulated based on measurement data [10]. Different models are derived for different geometries and species of vegetation [10]. There are 3 MED models. They are Weissberger, Fitted ITU-R and COST 235 [10].

2.4.1.1 Weissberger Model

One of the MED models was developed by Weissberger for predicting signal attenuation when the signal passes through the vegetation body at frequencies from 230 MHz to 96 GHz [12].

Weissberger's formula is given by [10]:

$$L\ (dB) = \begin{cases} 1.33 \times f^{0.284} d^{0.588} & 14m < d \leq 400m \\ 0.45 \times f^{0.284} d & 0m \leq d < 14m \end{cases} \quad (2.2)$$

where f is the frequency in GHz and d is depth of vegetation in meters.

Weissberger model is said to be suitable for frequencies up to 96 GHz [10], which includes some portion of mm-wave spectrum. However, this model is proven to be unsuitable for predicting vegetation attenuation at frequencies of mm-wave spectrum as it was found to predict path loss poorly at higher frequencies (11.2 GHz to 20 GHz) [12].

2.4.1.2 Fitted ITU-R Model

Fitted ITU-R (FITUR) model is the optimized version of previous ITU-R model derived using measurement results at 11.2 GHz and 20GHz [12].

The Fitted ITU-R model is given by [10]:

$$L\ (dB) = \begin{cases} 0.37 \times f^{0.18} d^{0.59} & out - of - leaf \\ 0.39 \times f^{0.39} d^{0.25} & in - leaf \end{cases} \quad (2.3)$$

where f is the frequency in MHz and d is depth of vegetation in meters.

2.4.1.3 COST 235 Model

The COST 235 model is given by [10]:

$$L\ (dB) = \begin{cases} 26.6 \times f^{-0.2} d^{0.5} & out - of - leaf \\ 15.6 \times f^{-0.009} d^{0.26} & in - leaf \end{cases} \quad (2.4)$$

where f is the frequency in MHz and d is depth of vegetation in meters.

2.4.1.4 Simulation of MED Models

Both of the FITUR model and COST 235 model has different formulas for out-of-leaf state and in-leaf state [10]. The different state of foliation is a characteristic of tree species in regions with temperate climate. The formulas for out-of-leaf condition are not applicable for tropical climate of Malaysia. Through software simulations as shown in Figure 2.3, it is evident that all three models have dual slope characteristic.

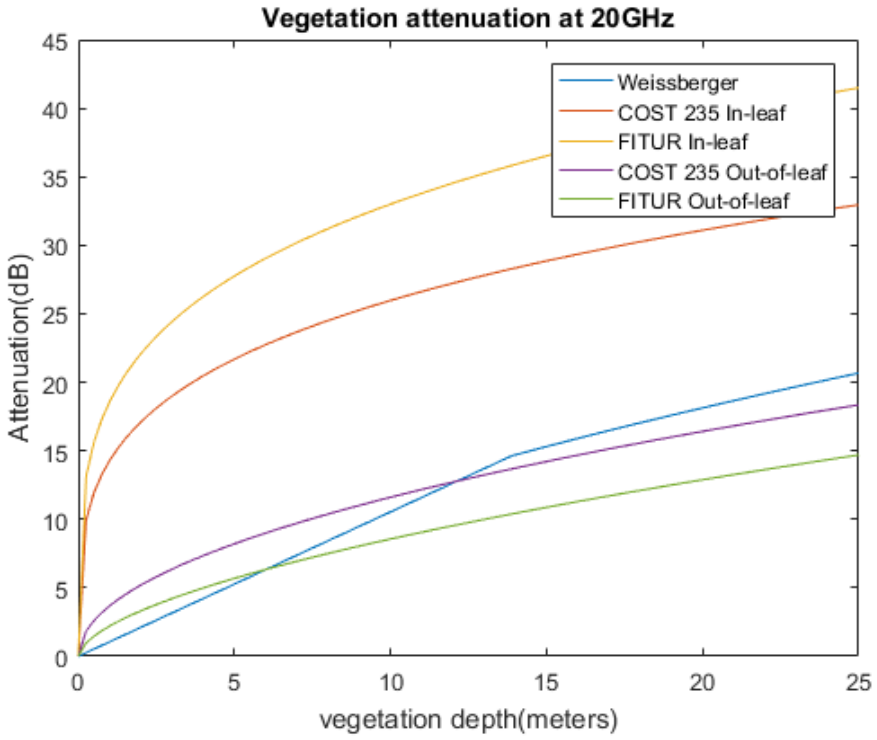

Figure 2.3: Vegetation attenuation versus depth curve at 20GHz for Weissberger, COST 235 (In-leaf and Out-of-leaf) and Fitted ITU-R (In-leaf and Out-of-leaf) at 20GHz

2.4.2 Modified Gradient Model

The Modified Gradient model is a subcategory of empirical model with parameters describing slopes of curve of vegetation attenuation (dB) against depth in vegetation (meters), which exhibits dual slope characteristic. This category of empirical model consists of three models namely: Maximum Attenuation (MA) model [15], Nonzero Gradient (NZG) model [15] and Dual Gradient model [12].

2.4.2.1 Maximum Attenuation Model

The Maximum Attenuation (MA) model is a model which is included in previous ITU-R recommendation. It is recommended for terrestrial link with one of the terminal located within woodland or forest and the other terminal located out of the vegetation [15]. It is given by [15]:

$$L(dB) = A_m[1 - \exp(-d\gamma/A_m)] \tag{2.5}$$

where A_m is maximum attenuation, d is length of path within woodland, γ is specific attenuation.

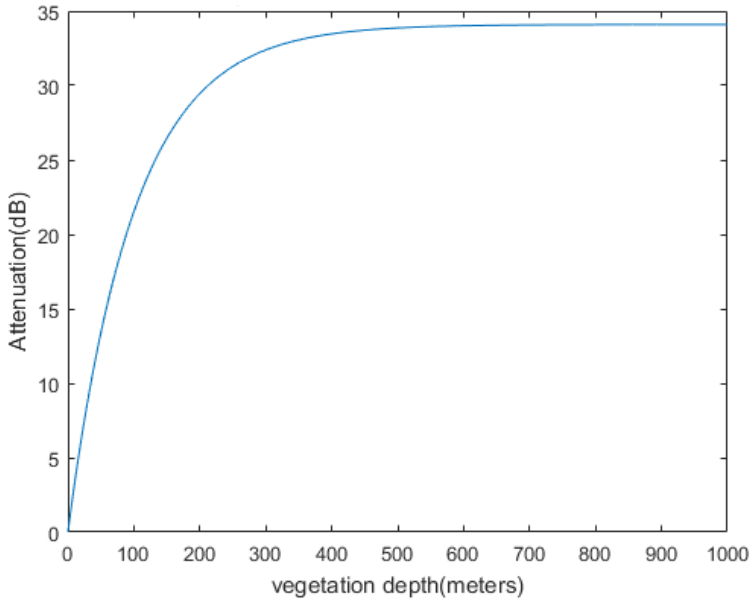

Figure 2.4: Maximum attenuation (MA) model at 2117MHz for mixed coniferous-deciduous vegetation

Based on software simulation as shown in Figure 2.4, it was found that attenuation (dB) against depth into vegetation (meters) curve of MA model has an initial steep slope and a zero slope at a longer depth. The initial slope is defined by a parameter known as specific attenuation which is fitted from measurement data [15]. In the recommendation, the specific attenuation for frequency between 30 MHz and 30 GHz are provided [15]. However, the specific attenuation may be different in practical scenarios as it is dependent on factors such as species, densities and water content of vegetative medium [15].

The maximum attenuation parameter is dependent on frequency [15]. The recommendation provides values of maximum attenuation for frequency up to 2117.5 MHz [15]. Besides from this lack of parameter data for frequencies of mm-wave spectrum, 5G does not have any propagation scenario where one terminal of the link is located within the forest. Furthermore, this model has a zero slope at longer depth as shown in Figure 2.4. This behaviour contradicts the dual slope characteristic. Therefore, this model is unsuitable for predicting effects of vegetation on mm-wave propagation.

2.4.2.2 Nonzero Gradient Model

The Nonzero Gradient (NZG) model is formulated to overcome zero gradient problem of Maximum Attenuation model [15]. It is given by [15]:

$$L(dB) = R_{\infty}d + k[1 - \exp\left(\frac{-(R_0 - R_{\infty})}{k}d\right)] \tag{2.6}$$

where R_0 is initial slope, R_{∞} is final slope, k is specific attenuation, d is vegetation depth in meters.

This model is recommended by previous ITU-R for predicting path loss due to vegetation at frequencies above 5 GHz [15]. It is derived from measurement data for frequencies between 9.6 GHz and 57.6 GHz [15]. In addition, the method to calculate both the slopes is provided in the recommendation [15].

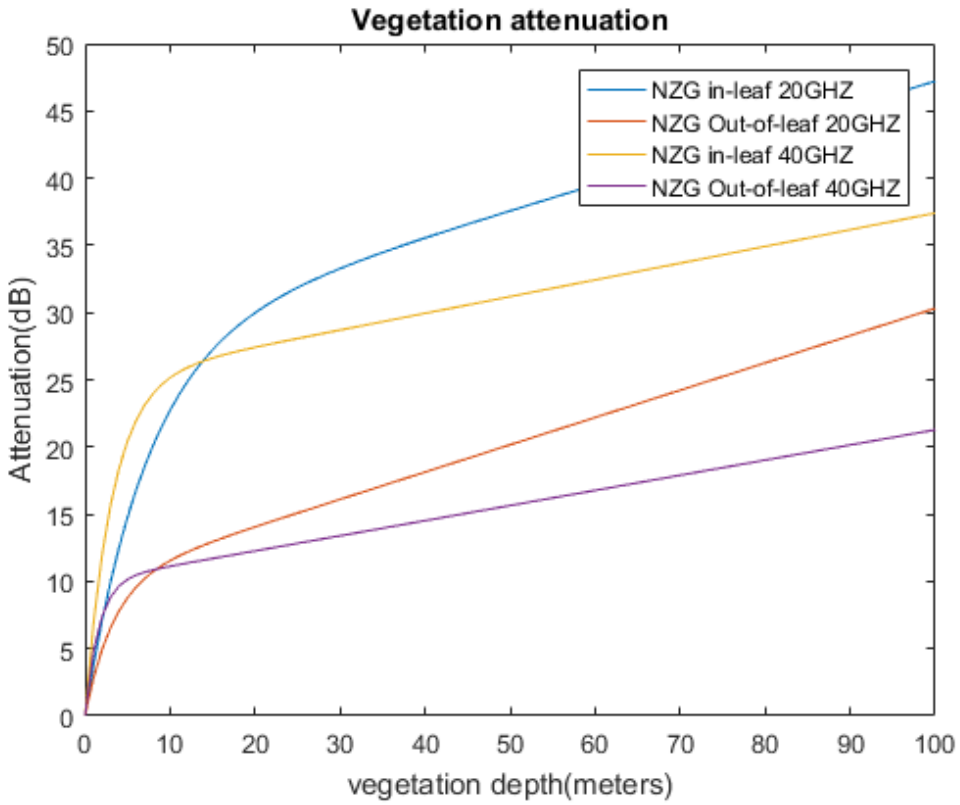

Figure 2.5: Vegetation attenuation versus depth curve at NZG model for in-leaf and out-of-leaf

The simulation in Figure 2.5 shows that NZG model has dual slope characteristic. According to Figure 2.5, the attenuation is higher at higher frequency and when the state of the tree is in-leaf state.

2.4.2.3 Dual Gradient Model

The Dual Gradient (DG) model is an enhancement of Nonzero Gradient model by taking into account of antenna beamwidth [12]. It is given by [12]:

$$L(dB) = \frac{R_\infty d}{f^a W^b} + \frac{k}{W_c}[1 - \exp\left(\frac{-(R_0 - R_\infty)}{k} W_c d\right)] \tag{2.7}$$

where R_0 is initial slope, R_∞ is final slope, k is specific attenuation, d is vegetation depth in meters, f is frequency in GHz, a, b, c are constants.

However, this model is inaccurate as its formula expresses an inverse relationship between attenuation and frequency [12]. In other words, as the frequency increases, the attenuation decreases [12].

2.5 Analytical Model

Analytical models are prediction models based on physics theories and take into account the underlying mechanism or physical processes of signal attenuation [14]. To analyse the signal attenuation of mm-wave due to vegetation, an analytical model based on Radioactive Energy Transfer (RET) theory was designed in 1985 [13].

Based on RET theory, the model assumes the vegetative medium as a statistically homogenous medium of random scatterers and absorbers [13]. It is characterized by a narrow forward lobe scatter function and an isotropic background [13].

The Radiative Energy Transfer theory is given by [12]:

$$s.\nabla I(\hat{r},\hat{s}) + (\sigma_A + \sigma_s) I(\hat{r},\hat{s}) = \frac{\sigma_s}{4\pi}\int_{4\pi} p(\hat{s},\hat{s}') I(\hat{r},\hat{s}') d\Omega' \tag{2.8}$$

where $\sigma_A$is absorption cross section per unit volume, σ_s is scatter cross-section per unit volume, $p(\hat{s},\hat{s}')$ is scatter function, I is specific intensity.

The RET model is the solution of above equation and is given by [12]:

$$L(dB) = -10\log_{10}\left(\begin{array}{ll} e^{-\tau} & I_{ri} \\ +\frac{\Delta\gamma_R^2}{4}\cdot\{[e^{-\hat{\tau}} - e^{-\tau}]\cdot\bar{q}_M + e^{-\tau}\cdot\sum_{m=1}^{M}\frac{1}{m!}(\alpha W\tau)^m\ [\bar{q}_m - \bar{q}_M]\} & I_1 \\ +\frac{\Delta\gamma_R^2}{2}\cdot\{-e^{-\hat{\tau}}\cdot\frac{1}{P_N} + \sum_{k=\frac{N+1}{2}}^{N}\ [A_k e^{-\frac{\hat{\tau}}{s_k}}\cdot\frac{1}{1-\frac{\mu_N}{s_k}}]\} & I_2 \end{array}\right) \tag{2.9}$$

where I_{ri} is coherent component, $I_1 + I_2$ are incoherent component, I_1 is forward scatter lobe, I_2 is isotropic background.

The RET theory expresses a dual slope characteristic for vegetation attenuation in dB against vegetation depth in meters [13]. The dual slope characteristic can be explained by the interplay of the coherent component and the incoherent component of the attenuated signal [13]. The coherent component has a well-defined direction of propagation [12]. It experiences absorption and scattering with a high attenuation rate at shorter depth into vegetation [12]. As a result of scattering, the incident wave is diffused with random or uncorrelated phases and dominates at longer depths [12]. The random phases of diffused wave are resulted from beam broadening of coherent component [11].

2.6 Summary of the Models and Model Selection

Table 2.2: Summary of the models and their characteristics

Models		Characteristics
Modified Exponential Decay Model		
1	Weissberger	• Simplicity • Dual slope characteristic
2	COST 235	
3	FITUR	
Modified Gradient Model		
1	Maximum Attenuation Model	• Does not display dual slope
2	Nonzero Gradient Model	• Display dual slope
3	Dual Gradient Model	• Attenuation inversely proportional to frequency
Analytical Model		
1	RET model	• Involves physical processes such as scattering and absorption • Display dual slope

The aim of the project is to investigate mm-wave propagation in an environment with presence of vegetative medium. As stated in Table 2.2, empirical models are

simplified and provide limited intuition of the background processes of vegetation attenuation. On the other hand, the RET model takes into account physical processes [14], which is a trait that all the empirical models do not have. Therefore, the RET model was selected.

2.7 Device-to-device Communications

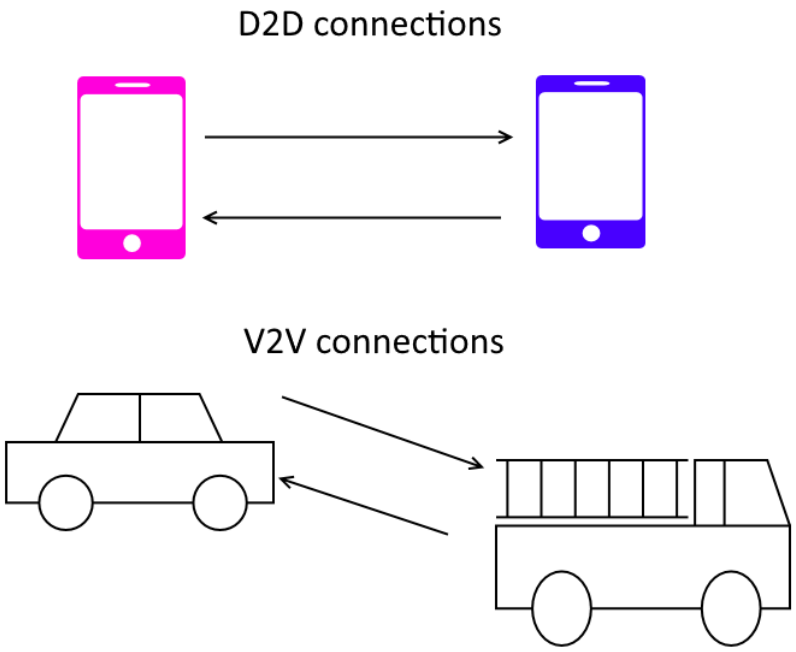

Figure 2.6: D2D and V2V connections

As shown in Figure 2.6, device-to-device (D2D) communication refers to direct communications between two mobile devices [16]. According to a METIS deliverable, D2D is important portion of modern radio communications [5]. It can be applied for public safety and commercial uses [16]. When both the communicating mobiles are in moving vehicles, the communication is known as vehicle-to-vehicle (V2V) connections [5].

CHAPTER 3 METHODOLOGY

This chapter provides details of the analytical model which was selected for investigating vegetation attenuation. The selected analytical model is RET model. It is part of a model which is included in Recommendation ITU-R P.833-8 [17]. The RET model predicts vegetation attenuation when the signal propagates through vegetation. The physical processes that were taken into account by RET model are through vegetation scattering and absorption [12]. The full ITU-R model excluding RET model takes into account a few other physical processes such as diffraction and ground reflection [17]. In the recommendation, the tree's crown is modelled as a cuboid as shown in the Figure 3.1 [17]. The software simulation was done using MATLAB.

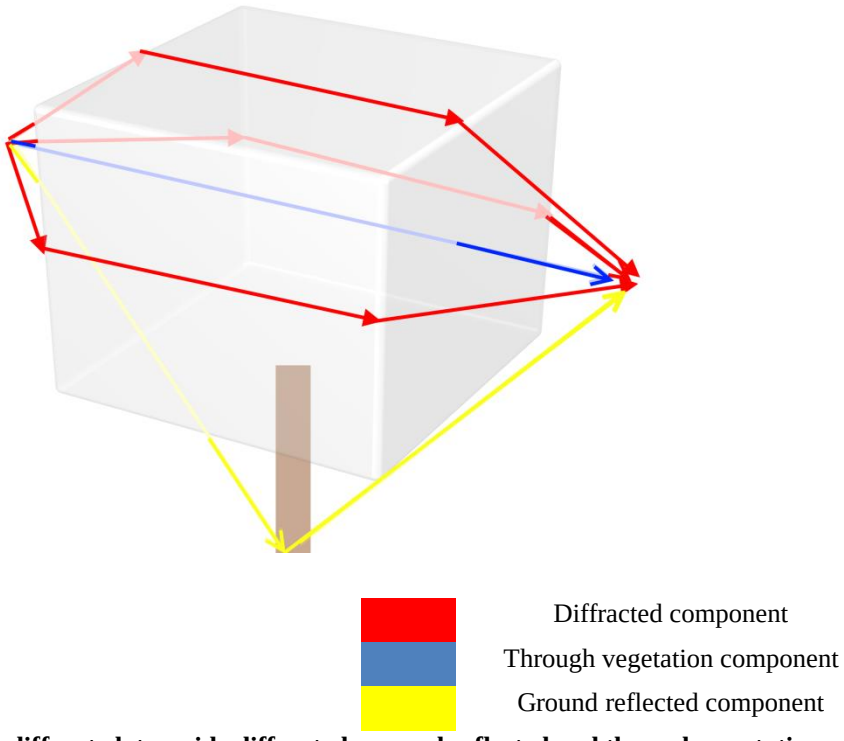

Figure 3.1: Top diffracted, two side diffracted, ground reflected and through vegetation components of the model

3.1 Through Vegetation Component

The through vegetation component of ITU-R model is the selected RET model [17]. It takes into account physical processes such as absorption and scattering [17]. The background of RET theory is provided in Section 2.5 of this project. This section focuses on how to implement this model.

RET model requires 4 input parameters [17]. These parameters are unique for each different combination of frequency (GHz) and tree species [17]. Tables consisting of values of these parameters are available in the ITU-R recommendation [17].

Table 3.1: 4 Input Parameters of RET Model

Parameters	Description
α	Forward scattered power / Total scattered power ratio
β	Beamwidth of forward lobe (degrees)
σ_τ	Combined scatter and absorption coefficient
W	Albedo

Signal attenuation due to forward scattering through the blocking vegetative medium is given by the following equation [17]:

$$L_{scat}(dB) = -10log_{10}\left(\begin{array}{c} e^{-\tau} + \\ \frac{\Delta\gamma_R^2}{4}\cdot\left\{\left[e^{-\hat{\tau}}-e^{-\tau}\right]\cdot\bar{q}_M + e^{-\tau}\cdot\sum_{m=1}^{M}\frac{1}{m!}(\alpha W\tau)^m[\bar{q}_m-\bar{q}_M]\right\} \\ +\frac{\Delta\gamma_R^2}{2}\cdot\left\{-e^{-\hat{\tau}}\cdot\frac{1}{P_N}+\sum_{k=\frac{N+1}{2}}^{N}\left[A_k e^{-\frac{\hat{\tau}}{S_k}}\cdot\frac{1}{1-\frac{\mu_N}{S_k}}\right]\right\} \end{array}\right) \quad (3.1)$$

where:

$\Delta\gamma_R = 0.6\cdot\Delta\gamma_{3dB}$ — 3dB beamwidth of receiving antenna

$\tau = (\sigma_a+\sigma_s)\cdot d$ — Optical density as function of distance, d

s_k	Attenuation coefficient
A_k	Amplitude factor

Other equations needed are [17]:

$$\bar{q}_m = \frac{4}{\Delta\gamma_R^2 + m\beta_S^2} \tag{3.2}$$

$$\beta_S = 0.6 \cdot \beta \tag{3.3}$$

$$P_N = sin^2\left(\frac{\pi}{2N}\right) \tag{3.4}$$

$$\hat{\tau} = (1 - \alpha W)\tau \tag{3.5}$$

Parameter m is the order of second row terms of (3.1). The suggested value of this parameter is 10 because values larger than 10 will not improve calculated answer significantly [17].

Next, the attenuation coefficients can be obtained by finding the roots of the following characteristic equation [17]:

$$\frac{\widehat{W}}{2} \cdot \sum_{n=0}^{N} \frac{P_n}{1 - \frac{\mu_n}{s}} = 1 \tag{3.6}$$

with:

$$P_n = \sin\left(\frac{\pi}{N}\right)\sin\left(\frac{n\pi}{N}\right), \qquad n = 1, \dots, N-1 \; and \; \widehat{W} = \frac{(1-\alpha)W}{1-\alpha W} \tag{3.7}$$

When n are 0 or N [17]:

$$P_N = P_n = sin^2(\frac{\pi}{2N}) \tag{3.8}$$

The characteristic equation has (*N+ 1)* roots and has following trait [17]:

$$s_{0,\ \ldots,\frac{N}{2}} = s_{N,\ \ldots,\frac{N+1}{2}} \tag{3.9}$$

N will affect the accuracy and computation efficiency of the algorithm [17]. Large *N* will result in better accuracy but increased complexity [17]. The increased complexity will result in longer time consumption to compute the answer [17]. A suggested tolerable range for *N* is 11 to 21 [17].

Comparison was made based on simulation results of different *N* within the range and no significant difference was observed. Therefore, *N* used in this project is 11 [17].

By using the attenuation coefficients obtained in preceding steps, one can obtain the amplitude factors by solving a system of linear equations. The equations are given by [17]:

$$\sum_{k=\frac{N+1}{2}}^{N} \frac{A_k}{1-\frac{\mu_n}{s_k}} = \frac{\delta_n}{P_N} \quad for\ n = \frac{N+1}{2} \ldots N \tag{3.10}$$

where:

$$\mu_n = -\cos(\frac{n\pi}{N}) \tag{3.11}$$

$$\delta_n = \begin{cases} 0\ for\ n \neq N \\ 1\ for\ n = N \end{cases} \tag{3.12}$$

By substituting calculated values of unknowns, distance and the 4 input parameters into (3.1), signal attenuation (dB) due to through vegetation component can be computed.

3.1.1 Band of Study and Input Parameters of Through Vegetation Component

The band of study is 37 to 40.5 GHz, which is one of the ITU-R selected bands [4]. The frequency of study is 37 GHz. For RET model or through vegetation component of the ITU-R model, parameters for 37 GHz and 61.5 GHz from mm-wave spectrum are available [17]. London Plane or *Plantanus hispanica muenchh* was selected for investigation because it is the only tree species with input parameters at 37 GHz and 61.5 GHz available in the recommendation document [17]. There are parameters for in-leaf state and out-of-leaf state [17]. Only parameters for in-leaf state were used in this project. The out-of-leaf state was not used because it is not suitable for tree species from tropical climate such as Malaysia. The parameters for London Plane are listed in Table 3.2.

Table 3.2: 4 Input Parameters of RET Model for London Plane at In-leaf State

Frequency(GHz)	α	β	σ_τ	W
37	0.95	18	0.441	0.95
61.5	0.25	2	0.498	0.50

3.2 Ground Reflection Loss

Ground reflection happens when a signal is reflected off of the ground near the vegetation as shown in Figure 3.2. The path loss due to ground reflection is given by [17]:

$$L_{ground} = 20log_{10}\left(\frac{d_1 + d_2}{d_0}\right) - 20log_{10}(R_0) \tag{3.13}$$

where R_0 is reflection coefficient, d_0 is direct distance between transmitter and receiver, d_1 is distance of transmitter from point of reflection and d_2 is distance of receiver from point of reflection.

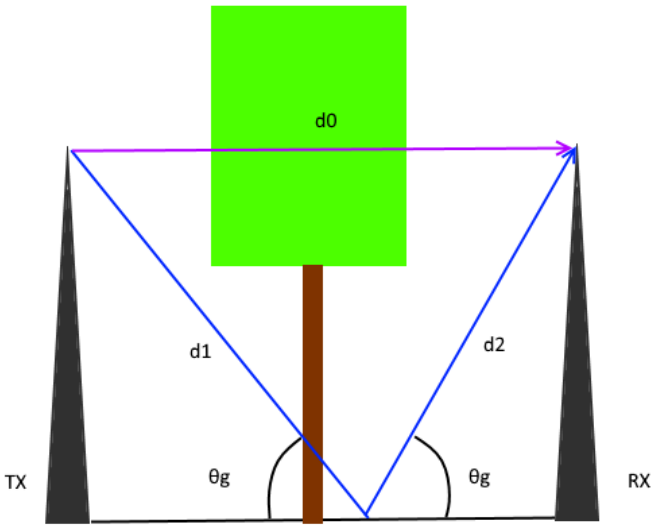

Figure 3.2: Ground reflected component

There are two types of polarization which includes horizontal polarization and vertical polarization. The formula for calculating reflection coefficient, R_0 is given by [17]:

$$R_{0,horizontal\ polarization} = \frac{\sin\theta_g - \sqrt{\eta - (cos\theta_g)^2}}{\sin\theta_g + \sqrt{\eta - (cos\theta_g)^2}} \tag{3.14}$$

$$R_{0,vertical\ polarization} = \frac{\sin\theta_g - \sqrt{\frac{\eta - (cos\theta_g)^2}{\eta^2}}}{\sin\theta_g + \sqrt{\frac{\eta - (cos\theta_g)^2}{\eta^2}}} \tag{3.15}$$

where θ_g is grazing angle and η is complex permittivity.

Complex permittivity, η is given by [18]:

$$\eta = \varepsilon_r - j60\lambda\sigma \tag{3.16}$$

where ε_r is relative permittivity, λ is wavelength, σ is conductivity.

3.2.1 Relationship of Reflection Coefficient and Grazing Angle

Ground under the vegetative medium may have different complex permittivity depending on its water content, which results in different reflection coefficient [19].The relative permittivity and conductivity for different surfaces such as wet ground, medium dry ground and dry ground are given in Recommendation ITU-R P.527 [17].

Table 3.3: Relative permittivity and conductivity for 3 ground surfaces at 37 GHz

Type of surface	Relative permittivity	Conductivity (S/m)
Dry ground	5	10
Medium dry ground	5	8
Wet ground	3	0.45

Using values in Table 3.3 and formulas in Section 3.2, the relationship between reflection coefficient and grazing angle on three surfaces including dry ground, medium dry ground and wet ground was investigated for both types of polarization.

3.2.2 Effects of Grazing Angle on Ground Reflection Loss for D2D Propagation

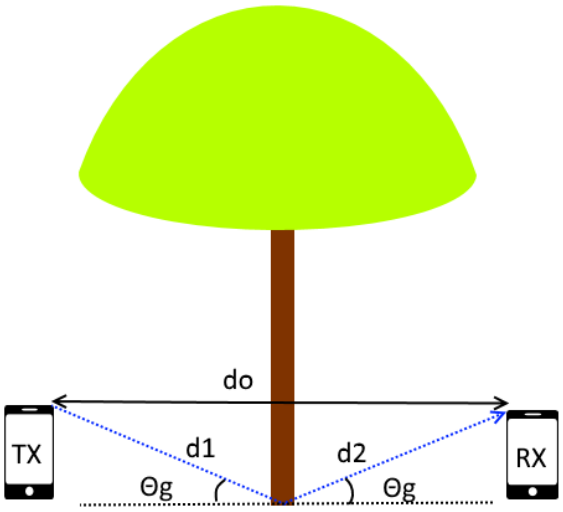

Figure 3.3: Ground reflection for D2D propagation

Figure 3.3 depicts a propagation scenario of D2D communication under a tree. The relationship between ground reflection loss, L_{ground} and grazing angle for D2D propagation can be investigated with a few assumptions:

- The distance of both transmitter and receiver from point of reflection is 3.5 m
- The link is perpendicular to the tree

The total distance of the receiving mobile from the transmitting mobile, d_0 is 7 m. Thus, an isosceles triangle with edges d_0,$d_1$and d_2 is formed. $d_1$and d_2 are of equal length. To study effects of grazing angle of on ground reflection, the parameters have to be in terms of grazing angle or constants. Using the sine rule and d_0 = 7 m, $d_1$and d_2 are given by:

$$d_1 = d_2 = \frac{\sin\theta_g \times 7}{\sin\,(180^0 - 2\theta_g)} \tag{3.17}$$

Substituting (3.17) to (3.13):

$$L_{ground} = 20log_{10}\left(\frac{2\sin\theta_g}{\sin\,(180^0 - 2\theta_g)}\right) - 20log_{10}(R_0) \tag{3.18}$$

Using (3.18) and formulas of reflection coefficient listed in Section 3.2, the relationship between ground reflection loss and grazing angle at 37 GHz was investigated.

3.3 Diffraction

There are three components of diffraction which includes top diffraction and side diffraction at the two edges of the crown of the tree, as shown in Figure 3.4 [17]. The diffractions are modelled as double isolated diffraction [17].

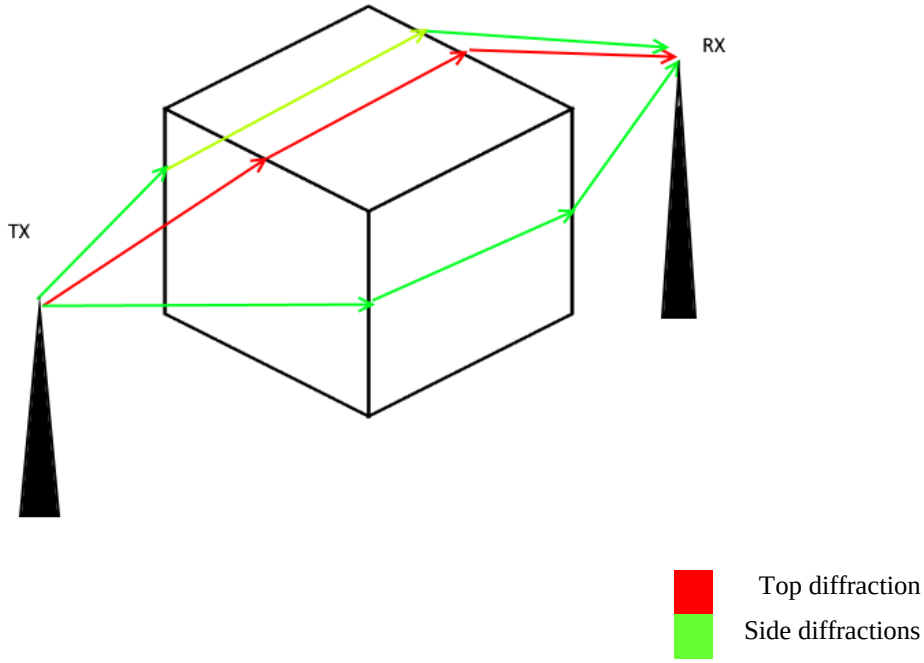

Figure 3.4: Diffracted components

3.3.1 Method of Calculation of Loss Due to Double Isolated Diffraction

The method to calculate double isolated diffraction is provided in Recommendation ITU-R P.526 [17]. By applying single knife edge diffraction at two successive points of diffraction, loss due to double isolated diffraction can be computed as follows [20]:

$$L = L_1 + L_2 + L_C \tag{3.19}$$

$$L_C = 10 \log \left[\frac{(a+b)(b+c)}{b(a+b+c)} \right] \tag{3.20}$$

Referring to Figure 3.5, L_1 is calculated using a, b and $h_1{}'$. L_2 is calculated using b, c and $h_2{}'$. Both L_1 and L_2 are modelled as single knife edge diffraction.

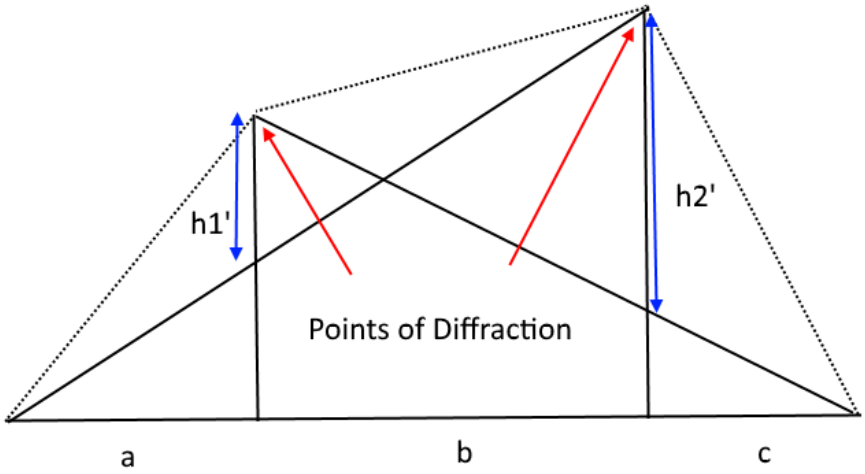

Figure 3.5: Double isolated diffraction

3.3.2 Method of Calculation of Loss Due to Single Knife Edge Diffraction

The method to calculate loss due to single knife edge diffraction is given in Recommendation ITU-R P.526 [20]. Calculation of loss due to single knife edge diffraction is as follow [20]:

$$J(v) = -20log\left(\frac{\sqrt{(1-C(v)-S(v))^2+(C(v)-S(v))^2}}{2}\right) \tag{3.21}$$

where $C(v)$ and $S(v)$ are the Fresnel cosine and sine integral. They are given by [20]:

$$C(v) = \int_0^v \cos\left(\frac{\pi s^2}{2}\right) ds \tag{3.22}$$

$$S(v) = \int_0^v \sin\left(\frac{\pi s^2}{2}\right) ds \tag{3.23}$$

v is given by [20]:

$$v = h\sqrt{\frac{2}{\lambda}\left(\frac{1}{d_1} + \frac{1}{d_2}\right)} \tag{3.24}$$

where h is height of top of obstacle to the straight line formed by joining the two ends of the path, d_1 and d_2 are distance from two ends to the obstacle as shown in Figure 3.6 [20].

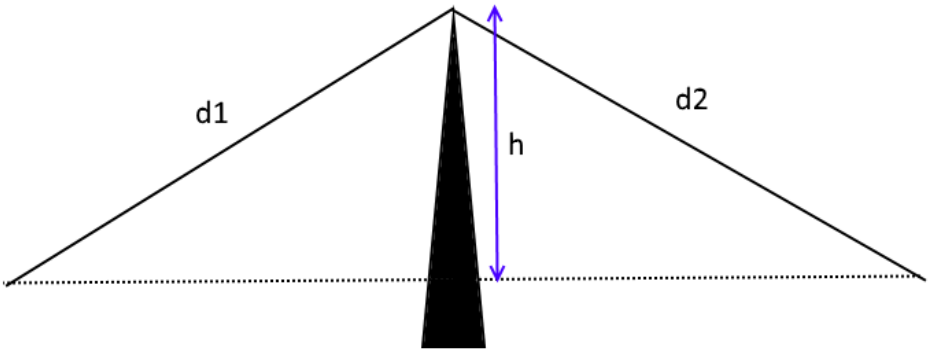

Figure 3.6: Single knife edge diffraction

3.3.3 Derivation of Top Diffracted Component

From the formulas listed in Section 3.3.1 and 3.3.2, the top diffracted component was derived along with knowledge on trigonometry. There are a few assumptions made for simplification:

- The crown of the vegetation is modelled as a cuboid [17].
- Both points of diffraction have the same height relative to base of crown.
- The heights of transmitter and receiver are shorter than the vegetation crown by $0.5t$ where t is the height of the crown as shown in Figure 3.7.
- Input parameters include a, b, c, t and wavelength.
- Position of the transmitter and receiver is always in line with each other. They are perpendicular to the cuboid crown's surfaces.

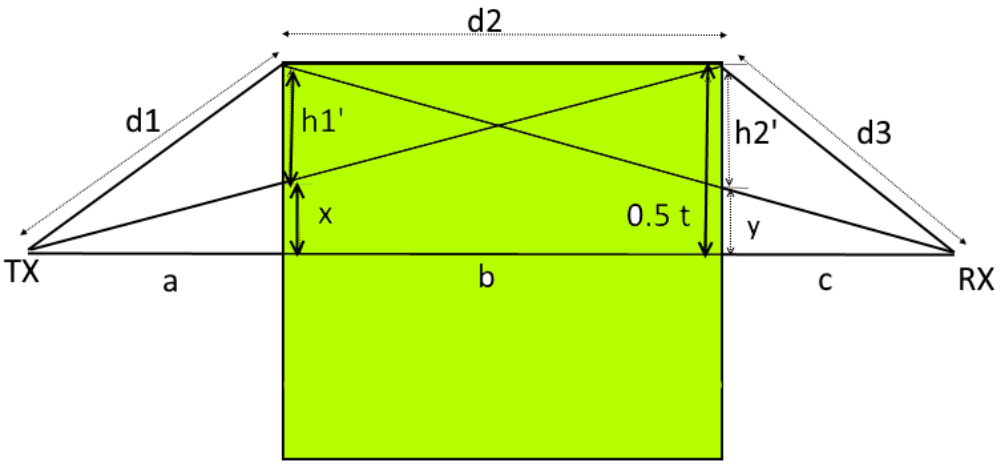

Figure 3.7: Top diffraction

The loss due top diffraction at the top of the crown is given by [20]:

$$L_{top} = L_1 + L_2 + L_C \tag{3.25}$$

where L_C is the correction term. It can be calculated with (3.20).

L_1 , the first single knife edge diffraction is given by:

$$L_1(v_1) = -20log\left(\frac{\sqrt{(1 - C(v_1) - S(v_1))^2 + (C(v_1) - S(v_1))^2}}{2}\right) \tag{3.26}$$

and v_1 is given by:

$$v_1 = h_1{}'\sqrt{\frac{2}{\lambda}(\frac{1}{d_1} + \frac{1}{d_2})} \tag{3.27}$$

where d_1, d_2 and $h_1{}'$ are as follows:

$$d_1 = \sqrt{(0.5t)^2 + a^2} \tag{3.28}$$

$$d_2 = b \tag{3.29}$$

$$x = 0.5t \times (\frac{a}{a+b}) \tag{3.30}$$

$$h_1' = 0.5t - x \tag{3.31}$$

L_2 , the first single knife edge diffraction is given by:

$$L_2(v_2) = -20log\left(\frac{\sqrt{(1 - C(v_2) - S(v_2))^2 + (C(v_2) - S(v_2))^2}}{2}\right) \tag{3.32}$$

with v_2, d_3 and h_2' as follows:

$$v_2 = h_2{}' \sqrt{\frac{2}{\lambda}(\frac{1}{d_2} + \frac{1}{d_3})} \tag{3.33}$$

$$d_3 = \sqrt{(0.5t)^2 + c^2} \tag{3.34}$$

$$y = 0.5t \times (\frac{c}{b+c}) \tag{3.35}$$

$$h_2' = 0.5t - y \tag{3.36}$$

where a is distance between transmitter and first diffraction point, b is distance between first and second diffraction point, c is distance between second diffraction point and receiver as shown in Figure 3.7.

3.3.4 Effects of Parameters *a, b* and *c* on Top Diffraction Loss

By setting frequency to 37 GHz and the height of crown to 3 m, the relationships between top diffraction loss and input parameters such as a , b and c were

investigated. When studying the effect of one input parameter on top diffraction loss, the parameter under investigation will be varied while the other parameters will be set to constants. The details these parameters for simulations are given in the following table.

Table 3.4: Details of parameters for simulations

Parameter under investigation	Other parameters
a	b is set to 3 m c is set to 10 m
b	a is set to 10 m c is set to 10 m
c	a is set to 10 m b is set to 3 m

In short, the distance of terminals from the points of diffraction (a and c) is 10 m and the tree is assumed to have a $3m \times 3m \times 3m$ cuboid crown. The assumption of a cuboid crown is necessary because all calculations are based on this assumption.

3.3.5 Side Diffracted Components

There are 2 side diffracted components as shown in Figure 3.8 [17]. The side to the left of the transmitter is side a [17]. The side to the left of it is side b [17]. The formulas for calculating attenuation caused by side diffracted components are given by [17]:

$$L_{side\ a} = L_{1a} + L_{2a} + L_C \tag{3.37}$$

$$L_{side\ b} = L_{1b} + L_{2b} + L_C \tag{3.38}$$

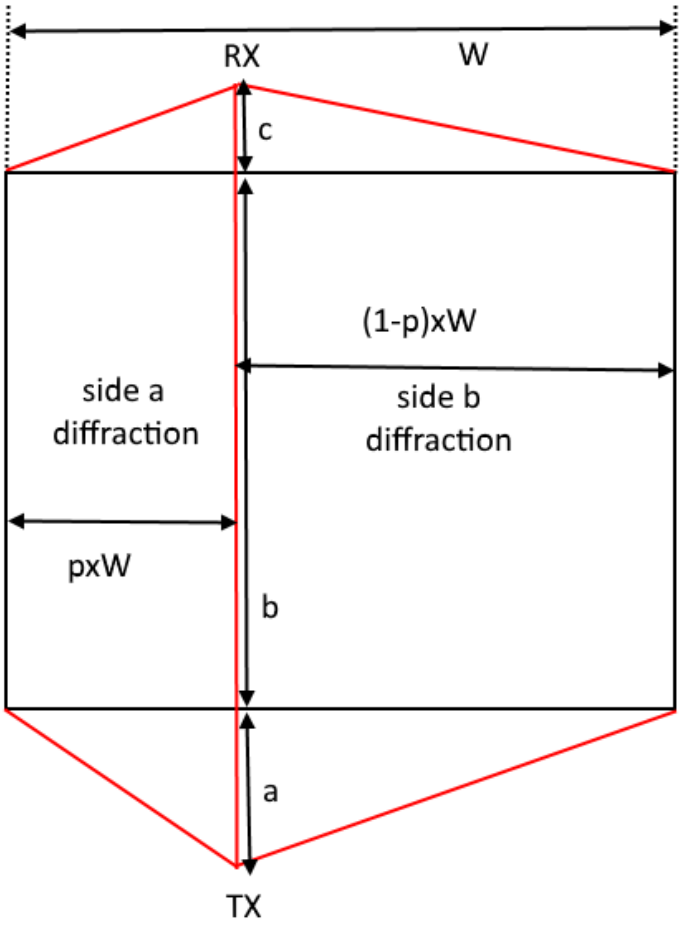

Figure 3.8: Side diffractions

3.3.6 Effects of Individual Width of Each Sides on Side Diffraction Loss

The method for computing (3.37) and (3.38) is similar to the method derived in Section 3.3.3 with some different notations.

$$L_{1a}(v_{1a}) = -20log\left(\frac{\sqrt{(1-C(v_{1a})-S(v_{1a}))^2+(C(v_{1a})-S(v_{1a}))^2}}{2}\right) \quad (3.39)$$

$$v_{1a} = h_{1a}'\sqrt{\frac{2}{\lambda}(\frac{1}{d_{1a}}+\frac{1}{d_{2a}})} \quad (3.40)$$

$$t_a = pW \quad (3.41)$$

$$t_b = (1-p)W \tag{3.42}$$

$$d_{1a} = \sqrt{{t_a}^2 + a^2} \tag{3.43}$$

$$d_{2a} = b \tag{3.44}$$

$$x = t_a \times (\frac{a}{a+b} \tag{3.45}$$

$$h'_{1a} = 0.5t - x \tag{3.46}$$

$$L_{2a}(v_{2a}) = -20log\left(\frac{\sqrt{(1-C(v_{2a})-S(v_{2a}))^2 + (C(v_{2a})-S(v_{2a}))^2}}{2}\right) \tag{3.47}$$

$$v_{2a} = {h_{2a}}'\sqrt{\frac{2}{\lambda}(\frac{1}{d_{2a}} + \frac{1}{d_{3a}})} \tag{3.48}$$

$$d_{3a} = \sqrt{{t_a}^2 + c^2} \tag{3.49}$$

$$y = t_a \times (\frac{c}{b+c}) \tag{3.50}$$

$$h'_{2a} = t_a - y \tag{3.51}$$

The formulas for side *b* can be obtained by changing notation *a* to *b*. The difference with top diffraction formulas is that instead of using $0.5t$, pW and $(1-p)W$ are used for individual widths of side *a* and side *b* respectively. W is the width of the cuboid crown and p is the fraction of width. The parameter, p is used to investigate the effects of side diffractions with different combinations of individual width. Based on Figure 3.9, a larger fraction of width, p of the crown will result in a larger width for side *a* and a smaller width for side *b* and vice versa.

An assumption to simplify the simulation algorithm is that the position of the transmitter and receiver is always in a straight line and perpendicular to the cuboid crown's surfaces.

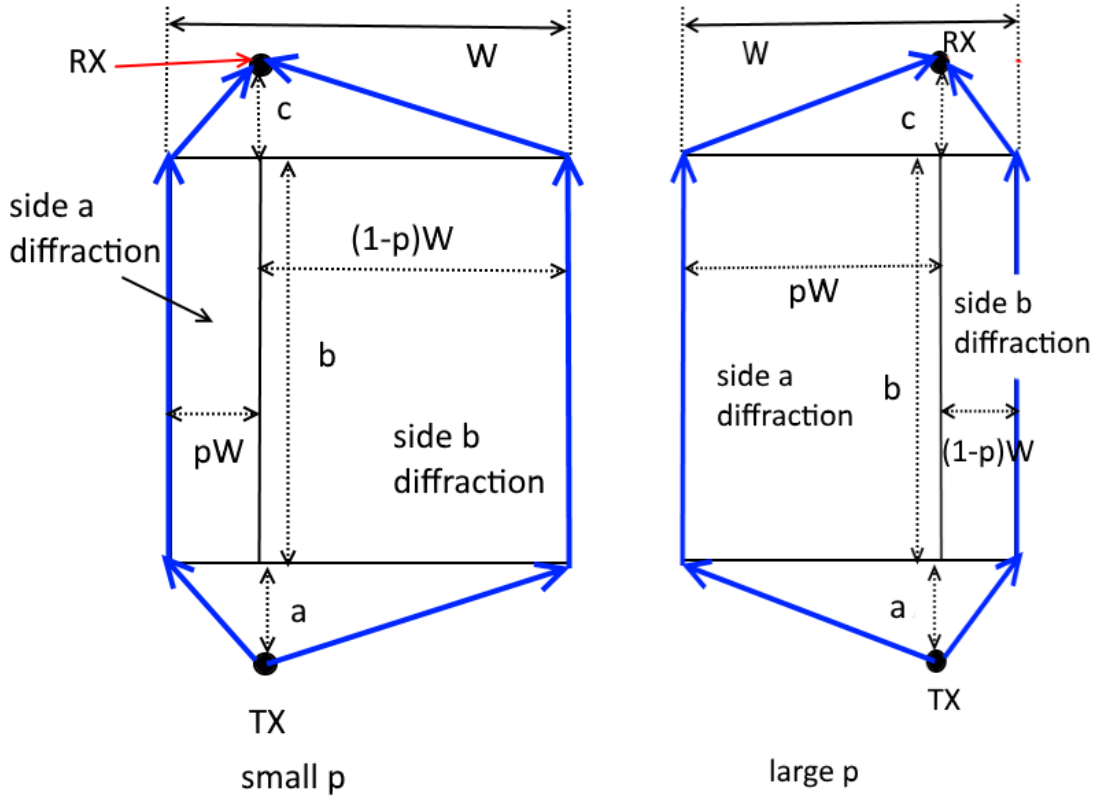

Figure 3.9: Side diffractions with small *p* and large *p*

By varying p, the positions of the transmitter and receiver relative to the cuboid crown change. When p is 1, the link is in line with right edge of the crown. On the other hand, the link is in line with left edge of the crown when p is 0. Thus, different combinations of positions of transmitter and receiver can be simulated. With W set to 3 m and setting the frequency as 37 GHz, a as 10 m, b as 3 m, c as 10 m, the relationship between the loss due to side diffracted components and the position of the terminals relative to the cuboid crown can be investigated.

3.3.7 Effects of Width of Crown on Side Diffraction Loss

In addition, by setting the frequency as 37 GHz, a as 10 m, b as 3 m, c as 10 m and p to 0.5, the relationship between loss due to side diffracted components and width of the crown was investigated using formulas stated in Section 3.3.6.

3.4 Software Simulation of the Model and Validation

The ITU-R model takes into account of physical processes such as through vegetation scattering, diffraction and ground reflection. It is a useful method to study mm-wave propagation in presence of vegetative medium. The methods are presented in the previous sections. They were implemented using MATLAB.

3.4.1 Validation of Through Vegetation Component

(3.6) is a characteristic equation and it has *(N+ 1)* roots. The roots have the following trait [17] :

$$S_{0,\ \ldots,\frac{N}{2}} = S_{N,\ \ldots,\frac{N+1}{2}} \tag{3.52}$$

The attenuation coefficients are valid if they fulfil above condition. The MATLAB code of RET model was validated by using this condition.

```
S =

  -1.050766553902012036558226029526 4
 -0.988358895010321963886571690959 56
 -0.887109790795228622587143539822 14
 -0.697237718112833080226701371907 15
 -0.444732732941910722522189309874 39
 -0.152752761719067350309301344736 92
  0.152752761719067230883602629174 65
  0.444732732941910608509535808285 49
  0.697237718112832964101659027245 89
  0.887109790795228547359726162495 51
  0.988358895010321961767487924209 44
   1.050766553902012024757393271640 8
```

Figure 3.10: The attenuation coefficients for London Plane at frequency of 37 GHz

Figure 3.10 is a snapshot of MATLAB command window displaying the attenuation coefficients for London Plane at 37 GHz. It fulfils the roots' condition. In addition, the plot (Figure 4.1) of attenuation (dB) against vegetation depth or distance into vegetation (meters) has two slopes as described in the literature. Thus, it was concluded that the code for this component is valid.

3.4.2 Validation of Ground Reflection Component

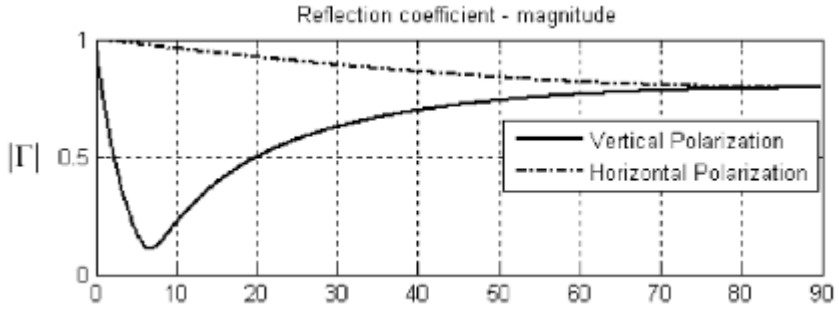

Figure 3.11: Sample plot of magnitude of reflection coefficient versus grazing angle from the book, Radar Signal Analysis and Processing Using MATLAB

Figure 3.11 is a MATLAB plot of magnitude of reflection coefficient versus grazing angle [21]. The plots (Figure 4.2 and Figure 4.3) of magnitude of reflection coefficient versus grazing angle are similar to the plot shown in Figure 3.11. This validates the MATLAB code for ground reflection component.

3.4.3 Validation of Diffraction Component

The base formulas for calculated are given in Section 3.3.1 and Section 3.3.2. The formulas in Section 3.3.3, 3.3.4, 3.3.5 and 3.3.6 were derived based on the aspects of mm-wave propagation that this project intends to investigate. Therefore, it was not possible to verify the codes.

3.5 Enhancement to Through Vegetation Component

In the recommendation, the tree crown is modelled as a cuboid for through vegetation component of ITU-R model [17]. Therefore, the relationship between the height of terminals (transmitter and receiver) and signal attenuation cannot be investigated. This is because signal attenuation remains the same even though the height varies because the depth in vegetation is constant for a cuboid crown [17]. Therefore, it results in a less realistic prediction of vegetation attenuation.

To address this problem, cuboid crown of through vegetation component of ITU-R model should be replaced by a solid shape that approximates crown of common vegetation causing signal attenuation. Considering an urban propagation environment, the tree species popular for urban tree planting in Kuala Lumpur, Malaysia were investigated.

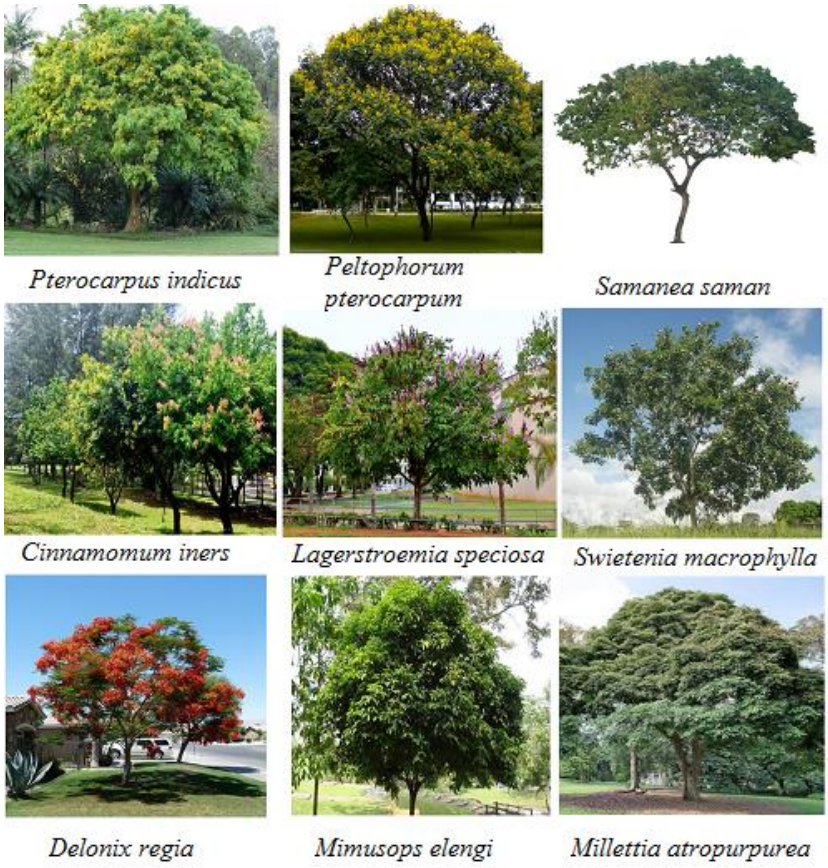

Figure 3.12 Tree species popular for urban tree planting in Kuala Lumpur

Then, solid shape of the crown was identified using eye estimation based on images of the trees shown in Figure 3.12 [22]. The urban tree species can be classified based on their crown shapes, such as hemispherical and spherical crown as listed in Table 3.5.

Table 3.5: Eye estimation of crown shape of tree species common for urban planting in Kuala Lumpur, Malaysia

Tree species	Canopy or crown by eye inspection
Pterocarpus indicus	Hemisphere
Peltophorum pterocarpum	Hemisphere
Samanea saman	Hemisphere
Cinnamomum iners	Sphere
Lagerstroemia speciosa	Hemisphere
Swietenia macrophylla	Sparsely spread sphere
Delonix regia	Hemisphere
Mimusops elengi	Sphere
Millettia atropurpurea	Hemisphere

Therefore, to investigate the effects of urban tree species in Kuala Lumpur, Malaysia, the through vegetation component will be enhanced to approximate crown shapes such as hemisphere and sphere.

3.5.1 Through Vegetation Component Considering a Hemispherical Crown

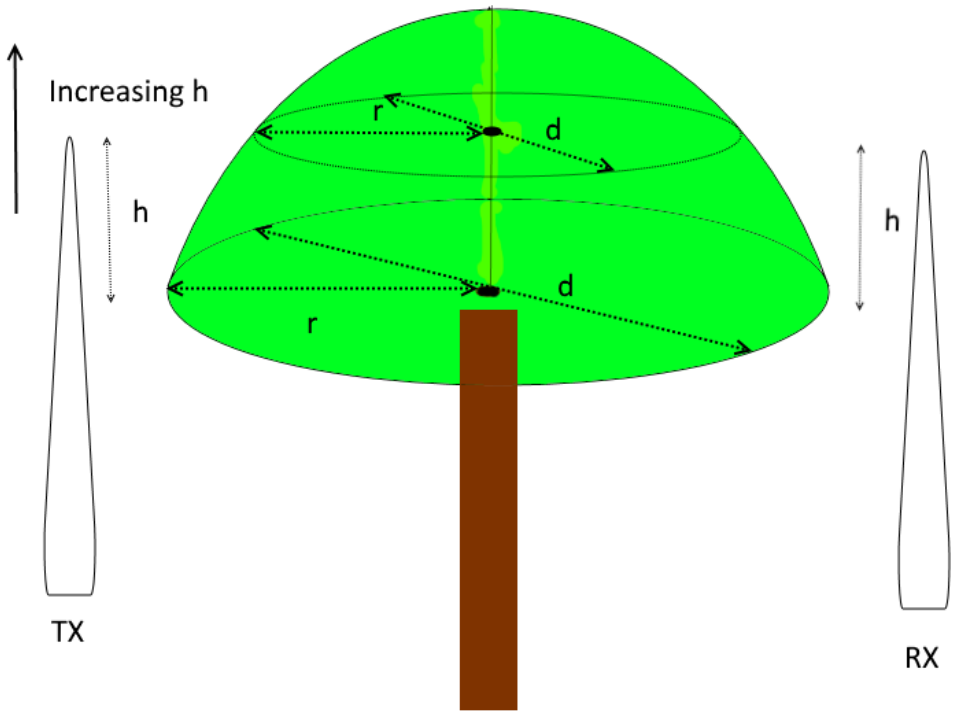

Figure 3.13: Vegetation's crown which is modelled as a hemisphere

Assumptions:

- Height of both terminals of the link are equal
- The vegetation geometry is same as London Plane at 37 GHz which means the same 4 input parameters listed in Table 3.2 will be used in simulation
- The link is perpendicular to the tree

The terminals of a link are transmitter and receiver. h is the height of the terminal relative to the base of the hemispherical crown. Referring to Figure 3.13, a circle can be formed when a plane parallel to the base of the crown intersects with the hemisphere. As the point of intersection becomes further away from the base of crown, the area of the circle formed will become smaller. r is the radius of these circles. d is the diameter of these circles. At the same time, d is depth in vegetation.

The relative height, h is a function of the depth in vegetation. The diameter of the circles decreases as h increases. Their relationship can be found with following derivations:

$$r^2 + h^2 = {r_w}^2 \tag{3.53}$$

$$r = \sqrt{{r_w}^2 - h^2} \tag{3.54}$$

$$d = 2r \tag{3.55}$$

$$d = 2\sqrt{{r_w}^2 - h^2} \tag{3.56}$$

$$h, d > 0 \tag{3.57}$$

where r_w is the radius of hemisphere tree crown.

By substituting these equations into (3.1) and assuming a tree crown with diameter of 3 m, the effects of tree species with hemispherical crown on mm-wave propagation were investigated.

3.5.2 Through Vegetation Component Considering a Spherical Crown

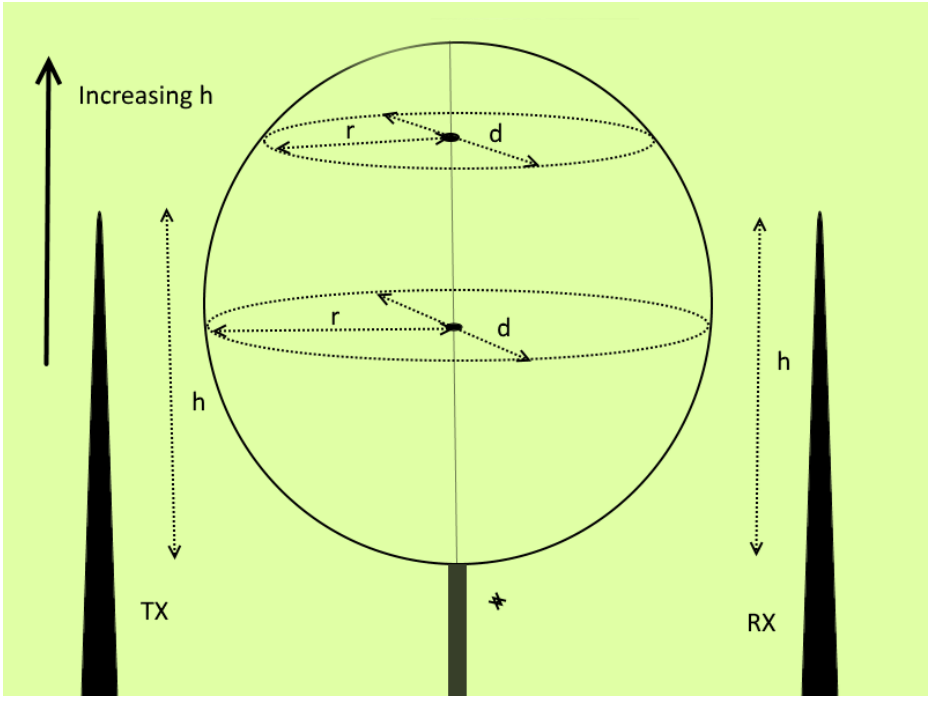

Figure 3.14: Vegetation's crown which is modelled as a sphere

Some of tree species that were planted for urban greening have spherical crown. To model crown of these species as shown in Figure 3.14, some assumptions were made:

- Height of both terminals of the link are equal
- The vegetation geometry is same as London Plane at 37 GHz which means the same 4 input parameters listed in Table 3.2 will be used in simulation.
- The link is perpendicular to the tree

Besides that, relative height, h is the height of the terminal relative to the bottom of the spherical crown. As the relative height increases, the area of the circle will change. r is the radius of the circles which are formed as relative height changes. d is the diameter of these circles. At the same time, d is also the depth in vegetation. As shown in Figure 3.14, the vegetation depth changes as the relative height changes.

The relative height, h is a function of the depth in vegetation. Their relationship can be described with following equations:

$$h = \sqrt{{r_w}^2 - r^2} + r_w \tag{3.58}$$

$$r^2 + (h - r_w)^2 = {r_w}^2 \tag{3.59}$$

$$d = 2r \tag{3.60}$$

$$d = 2\sqrt{{r_w}^2 - (h - r_w)^2} \tag{3.61}$$

$$h, d > 0 \tag{3.62}$$

where r_w is the radius of spherical tree crown.

Substituting these equations back into (3.1) and assuming a tree with diameter of 3 m, the effects of tree species with spherical crown on mm-wave propagation were investigated.

3.5.3 Comparison between Enhanced Model and Original Model

Section 3.5.1 and 3.5.2 describes proposed methods to account for crown shape such as hemisphere and sphere. This section presents a way to compare signal attenuation caused by vegetation with hemispherical crown, spherical crown and the original

model's cuboid crown shape. To compare between enhanced RET model and the original through vegetation component of ITU-R model, the volume of vegetation is kept constant.

Assume a tree crown with vegetation depth of 3 m, the volume of vegetation for a tree with cuboid crown is given by:

$$V = d^3 = 3^3 = 27\ m^3$$

A hemispherical crown with volume of $27m^3$ has radius of:

$$V = \frac{2}{3}\pi r^3$$

$$r = 2.34\ m$$

A spherical crown with volume of $27m^3$ has radius of:

$$V = \frac{4}{3}\pi r^3$$

$$r = 1.86\ m$$

Using formulas in Section 3.5.1 and 3.5.2 and (3.1), the comparison between the enhanced model and original model can be implemented.

CHAPTER 4 DATA PRESENTATION AND DISCUSSION

4.1 Through Vegetation Component for 37 GHz and 61.5 GHz

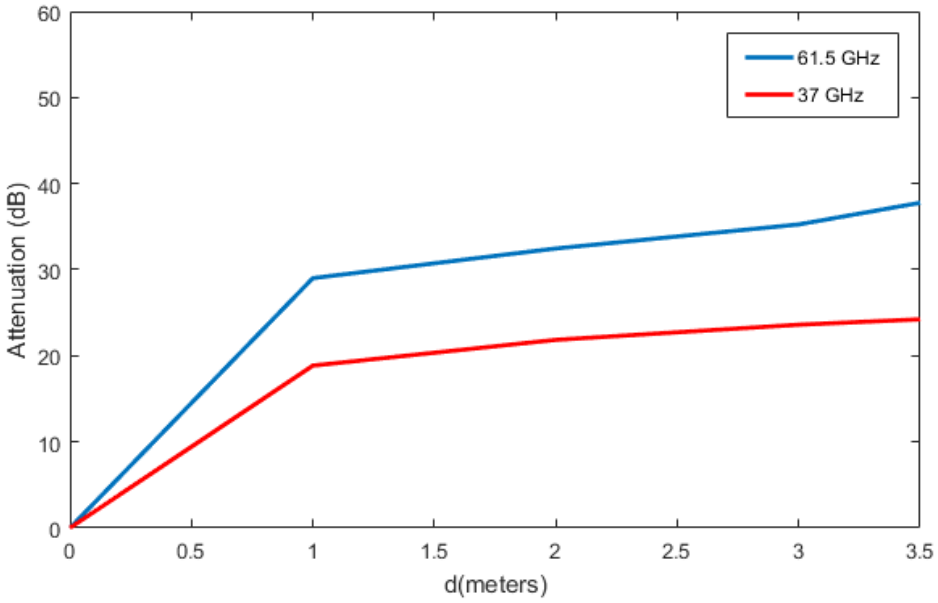

Figure 4.1: Through vegetation attenuation (dB) against depth into vegetation (meters) for in-leaf London Plane tree species at frequencies of 37GHz and 61.5GHz

Attenuation (dB) against depth into vegetation (meters) curves in Figure 4.1 shows that through vegetation attenuation at 37 GHz is lower than that of 61.5 GHz. Through vegetation attenuation takes into account absorption loss and scattering when the signal propagates in the vegetation [12]. At higher frequencies, the signal attenuation due to scattering and absorption is higher. This means that at higher frequencies, signal experiences more scattering and absorption loss. This characteristic of signal can be explained by the fact that signals at higher frequencies have shorter wavelengths. As the wavelength becomes shorter, the ratio of size of leaf of the tree to the wavelength increases. As a result, the probability of a signal experiencing scattering increases. Besides that, both the curves in Figure 4.1 display dual slope characteristic. Both of the curves show a steeper slope followed by a less steep slope. According to both of curves in Figure 4.1, the signal attenuation increases as depth into vegetation increases. The attenuation rate is higher at 0 m to 1 m. After 1 m, the attenuation rate falls but it is still a positive slope. This behaviour is

due to interchanging role of coherent component and incoherent component which is described in Section 2.5.

4.2 Reflection coefficient

This section discusses the relationship between reflection coefficient and grazing angle for both horizontal polarization and vertical polarization at 37 GHz. It is investigated over several surfaces such as dry ground, medium dry ground and wet ground. The details and the formulas are available at Section 3.2.

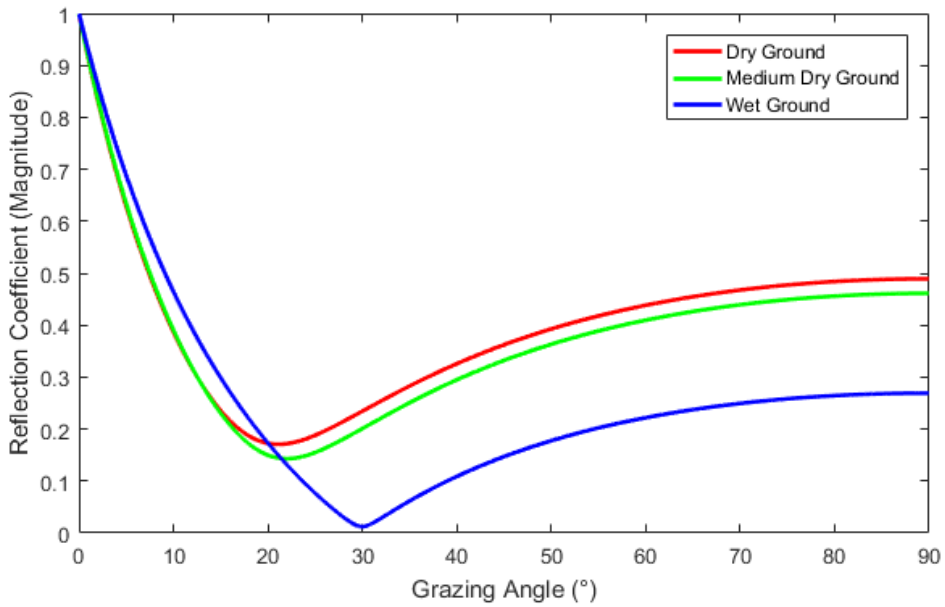

Figure 4.2: Magnitude of reflection coefficient versus grazing angle for vertical polarization at 37 GHz for different type of ground surface.

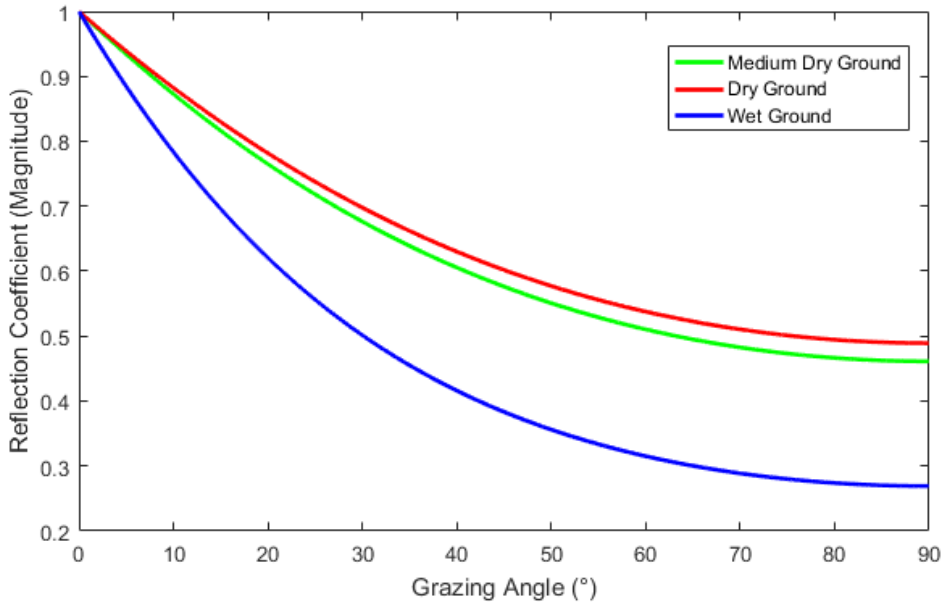

Figure 4.3: Magnitude of reflection coefficient versus grazing angle for horizontal polarization at 37 GHz for different type of ground surface.

Figure 4.2 shows the relationship between magnitude of reflection coefficient and grazing angle at 37 GHz for surfaces such as dry ground, medium dry ground and wet ground for vertical polarization. At grazing angles less than 20 º, the wet ground surface has the largest magnitude of reflection coefficient when compared to dry ground and medium dry ground. Beyond 20 º, wet ground has the smallest magnitude of reflection coefficient. The magnitudes of reflection coefficient of dry ground and medium dry ground are different by around 0.1 for grazing angle ranging from 0 º to 90 º based on eye estimation.

Figure 4.3 shows the relationship between magnitude of reflection coefficient and grazing angle at 37 GHz for surfaces such as dry ground, medium dry ground and wet ground for horizontal polarization. The magnitude of reflection coefficient decreases as the grazing angle increases for all surfaces. Relative to dry ground and medium dry ground, wet ground has the smallest magnitude of reflection coefficient for grazing angle ranging from 0 º to 90 º.

4.3 Attenuation due to Ground Reflection

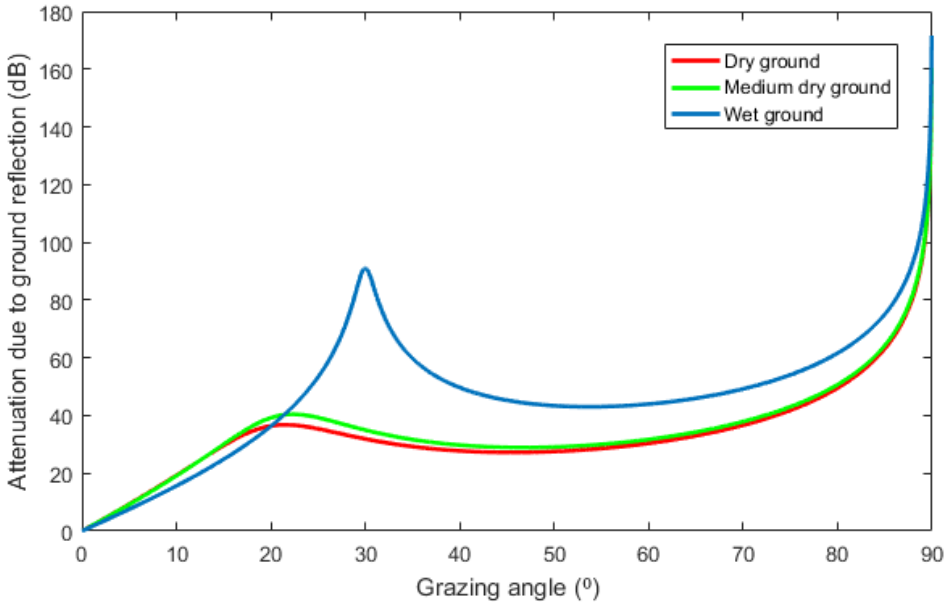

Figure 4.4: Attenuation due to ground reflection versus grazing angle for vertical polarization at 37 GHz for different type of ground surface.

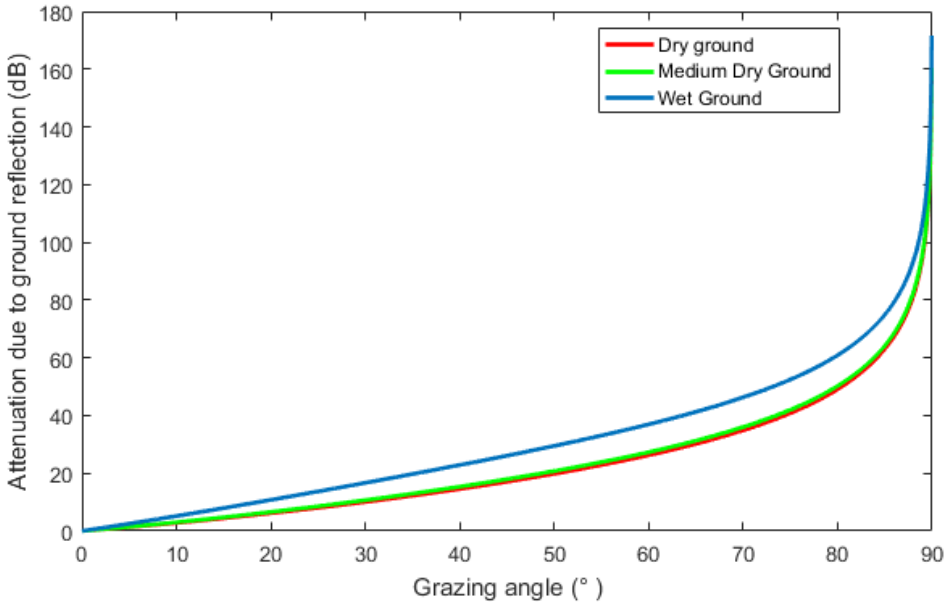

Figure 4.5: Attenuation due to ground reflection versus grazing angle for horizontal polarization at 37 GHz for different type of ground surface.

Figure 4.4 shows the plots of attenuation due to ground reflection (dB) versus grazing angle for 3 ground surfaces for vertical polarization. From around 20 º to 90 º, wet ground has the largest attenuation when compared to dry ground and medium dry ground. It peaks at around 30 º with an attenuation of 90 dB. For dry ground and medium dry ground, the attenuation peaks at around 20 º.

Figure 4.5 shows the plots of attenuation due to ground reflection (dB) versus grazing angle for 3 ground surfaces for horizontal polarization. The attenuation increases from 0 dB to over 100 dB as the grazing angle increases. This trend is similar for all 3 ground surfaces. Wet ground has the largest attenuation when compared to dry ground and medium dry ground.

Generally, the attenuation due to ground reflection is much smaller at smaller grazing angle.

4.4 Effects of Parameters *a, b* and *c* on Top Diffraction Loss

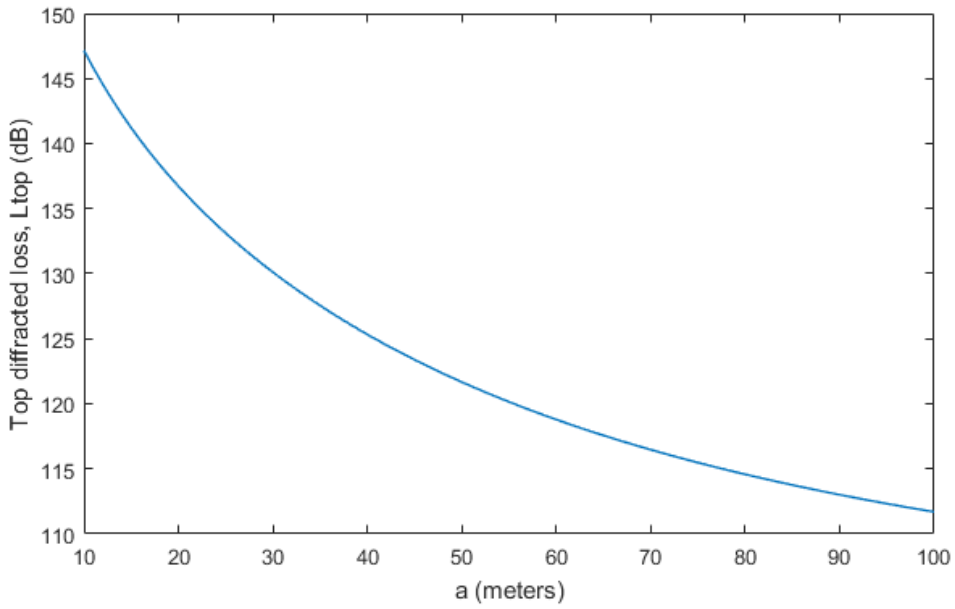

Figure 4.6: Top diffraction loss versus distance between transmitter and first diffraction point, *a* (meters) at 37 GHz

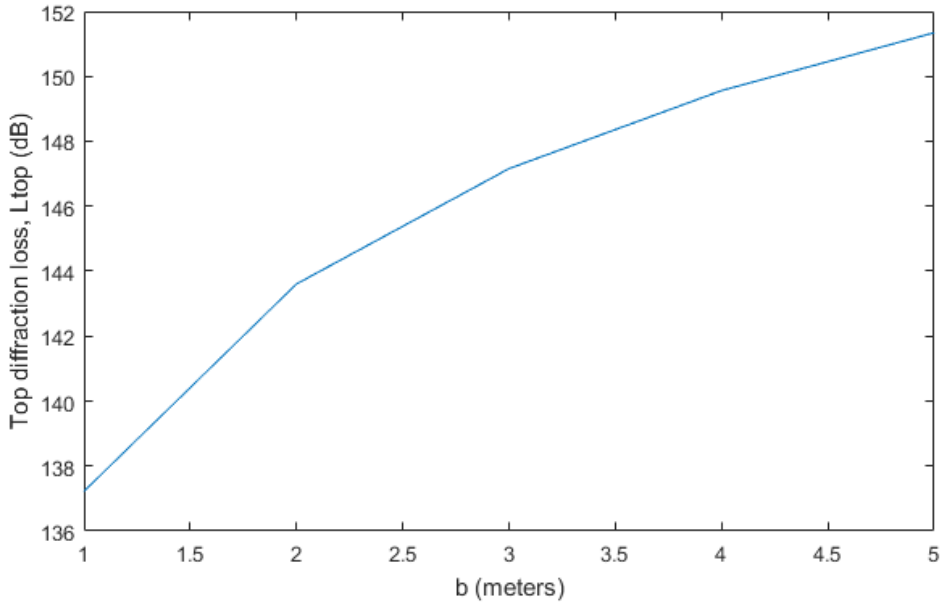

Figure 4.7: Top diffraction loss versus distance between first and second diffraction point, *b* (meters) at 37 GHz

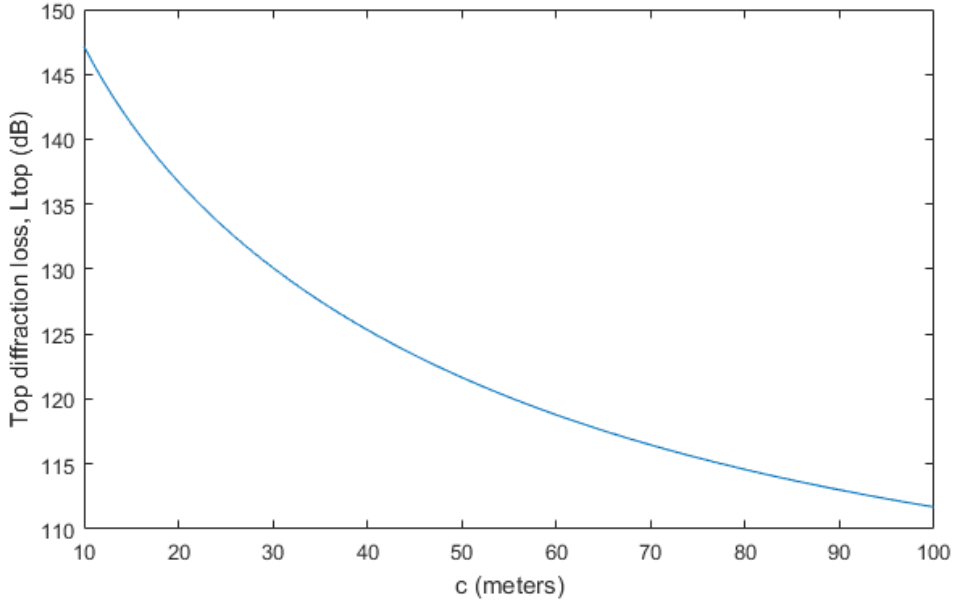

Figure 4.8: Top diffraction loss versus distance between second diffraction point and receiver, *c* (meters) at 37 GHz

Figure 4.6 shows the relationship between the top diffraction loss and the distance between transmitter and first diffraction point, *a* at 37 GHz. Figure 4.8 shows the relationship between the top diffraction loss and the distance between second

diffraction point and receiver, c at 37 GHz. Through eye estimation, it is clear that their curves are identical. The loss due to top diffraction decreases as distance between transmitter and first diffraction point, a or the distance between second diffraction point and receiver, c increases. This means the loss due to diffraction is smaller as the transmitter and the receiver are more distant from the tree which causes diffraction. According Figure 4.6 and Figure 4.8, the loss is still over 100 dB even when a and c are 100 m. This order of attenuation is much larger than through vegetation attenuation at 37 GHz shown in Figure 4.1. Figure 4.7 shows the relationship between top diffraction loss and the distance between both the diffraction points. The distance between both the diffraction points refers to the width of tree. The loss increases from around 137 dB to around 151 dB as the distance between both points of diffraction increases from 1 m to 5 m.

In short, diffraction loss is much larger than through vegetation attenuation at 37 GHz.

4.5 Effects of Individual Width of Each Sides on Side Diffraction Loss

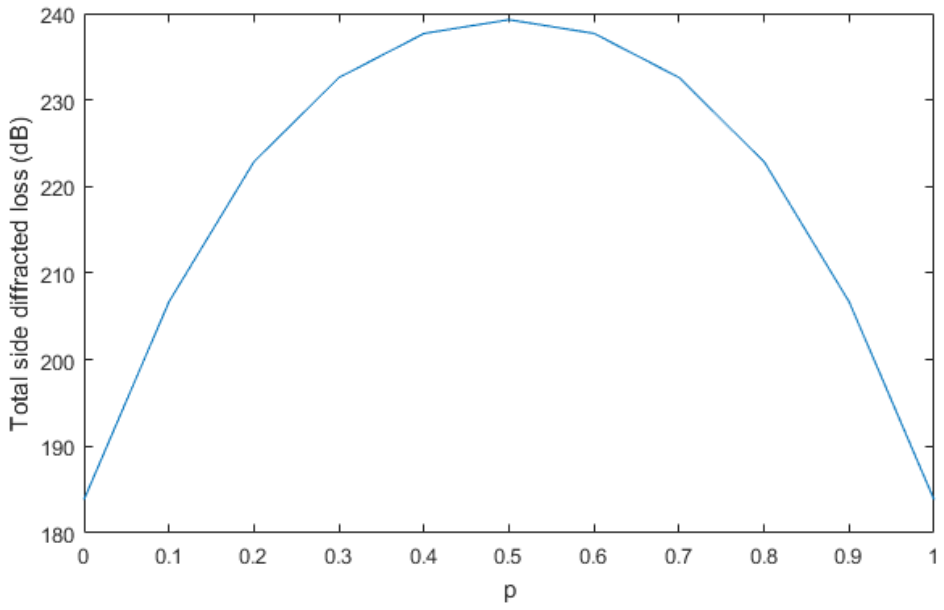

Figure 4.9: Total side diffracted loss versus fraction of width, *p* at 37 GHz

Figure 4.9 shows that the total side diffracted loss is minimal at 185 dB when p is 0 or 1, when the link is at right or left edges of the cuboid crown. The total side diffracted loss is maximal at 240 dB when p is 0.5, which is when the link of transmitter and receiver is located in the middle of the crown. Based on the observation, the total side diffracted loss is larger when the combination of widths of side a and side b are close to each other. The total side diffracted loss is smaller when the width of one side is wider than the other side. In other words, the loss is smaller when the positions of transmitter and receiver are closer to either left edge or right edge of the crown.

4.6 Effects of Width of Crown on Side Diffraction Loss

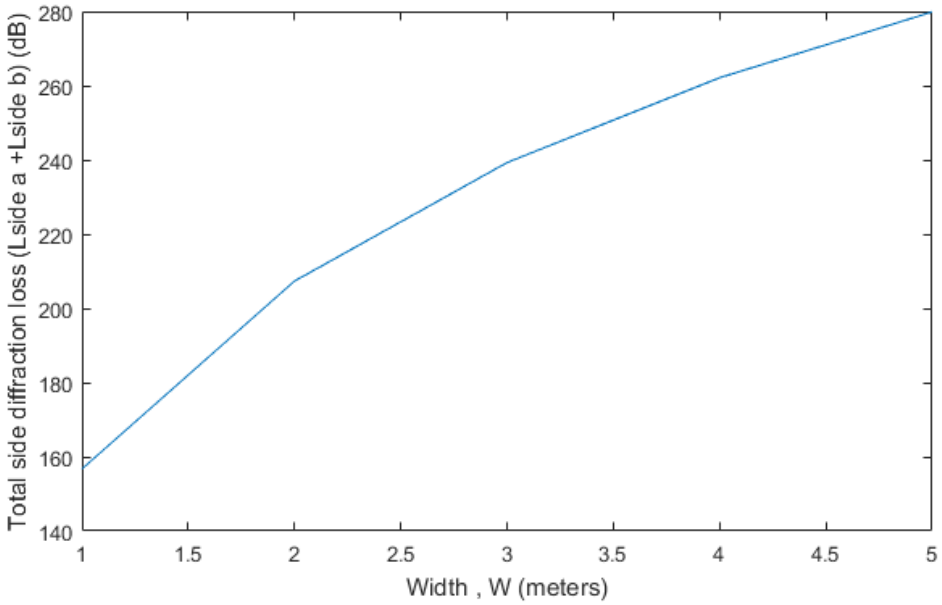

Figure 4.10: Total side diffracted loss versus width of crown at 37 GHz

Figure 4.10 shows the relationship between total side diffracted loss and total width of the crown. The total side diffracted loss increases from around 160 dB to 280 dB as total width of the crown increases from 1 m to 5 m.

4.7 Through Vegetation Component Considering a Hemispherical Crown

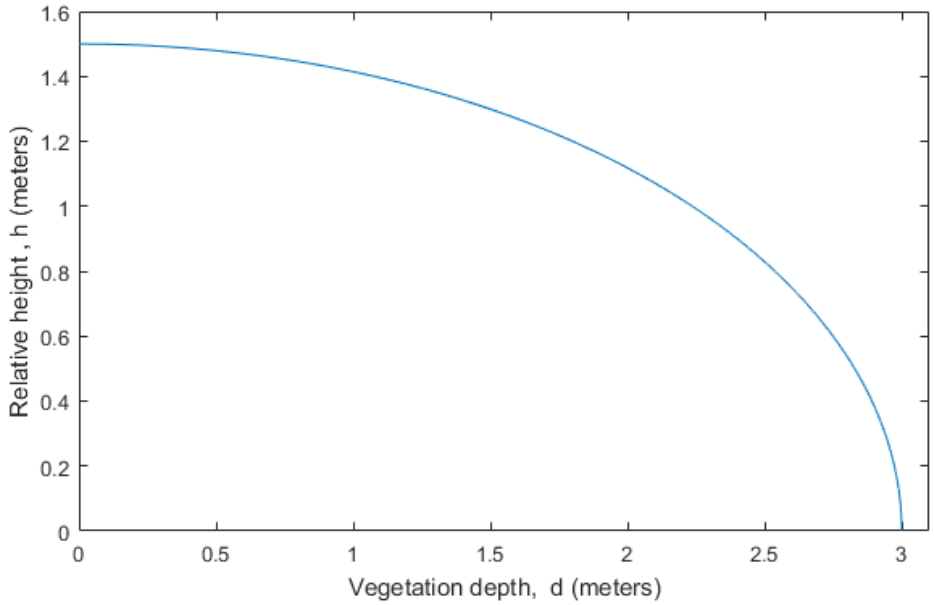

Figure 4.11: Relative height versus vegetation depth at 37 GHz considering a hemispherical crown

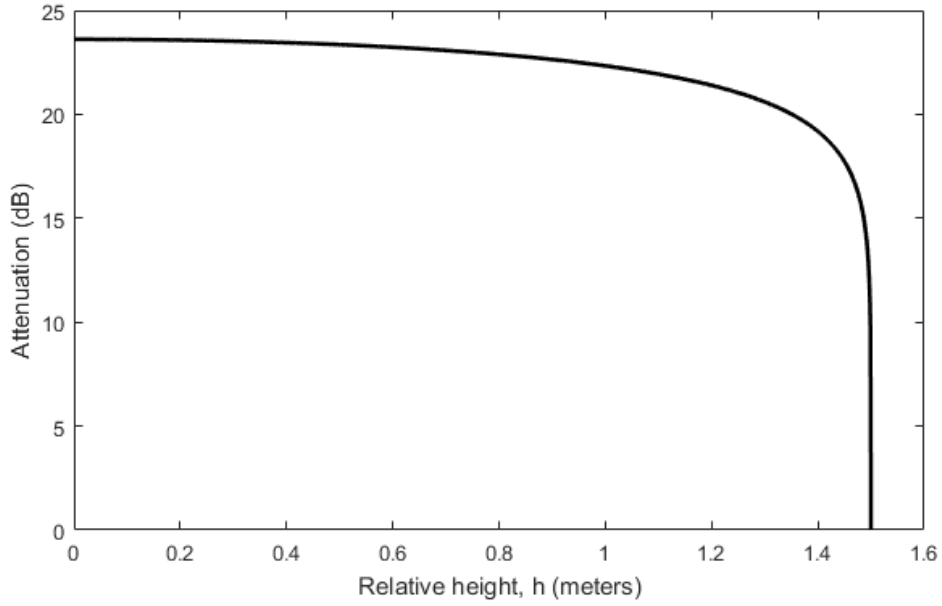

Figure 4.12: Through vegetation attenuation versus relative height at 37 GHz considering a hemispherical crown

Figure 4.11 shows the relationship between relative height and vegetation depth for a tree crown modelled as a hemisphere. Relative height refers to height of transmitter and receiver relative to the base of crown. Vegetation depth is a term for the diameters of the circles formed when parallel planes intersected with the hemisphere. Its value changes as relative height varies. According to Figure 4.11, vegetation depth is longest when relative height is zero, at the base of the crown, which is the largest circle of all circles formed. The vegetation depth decreases as the relative height increases.

Figure 4.12 shows the relationship between through vegetation attenuation and relative height. London Plane's parameters at 37 GHz were used as input parameters during this simulation since it is the only species with values of parameters at 37 GHz provided in the recommendation [17]. According to Figure 4.12, the through vegetation attenuation for a hemispherical crown decreases with a very slow rate from about 24 dB to around 20 dB as relative height varies from 0 to about 1.4 m. Beyond 1.4 m, the attenuation decreases with a steep slope from around 20 dB to 0 dB at 1.5 m.

As the relative height increases, vegetation depth decreases. As the vegetation depth decreases, signal attenuation decreases. It shows that through vegetation attenuation is proportional to vegetation depth for a tree with hemispherical crown.

4.8 Through Vegetation Component Considering a Spherical Crown

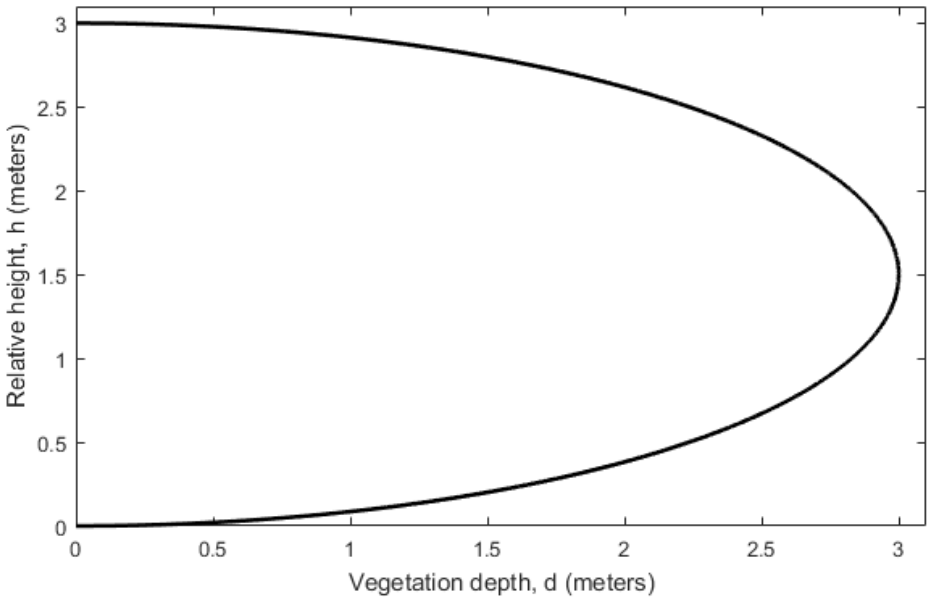

Figure 4.13: Relative height versus vegetation depth at 37 GHz considering a spherical crown

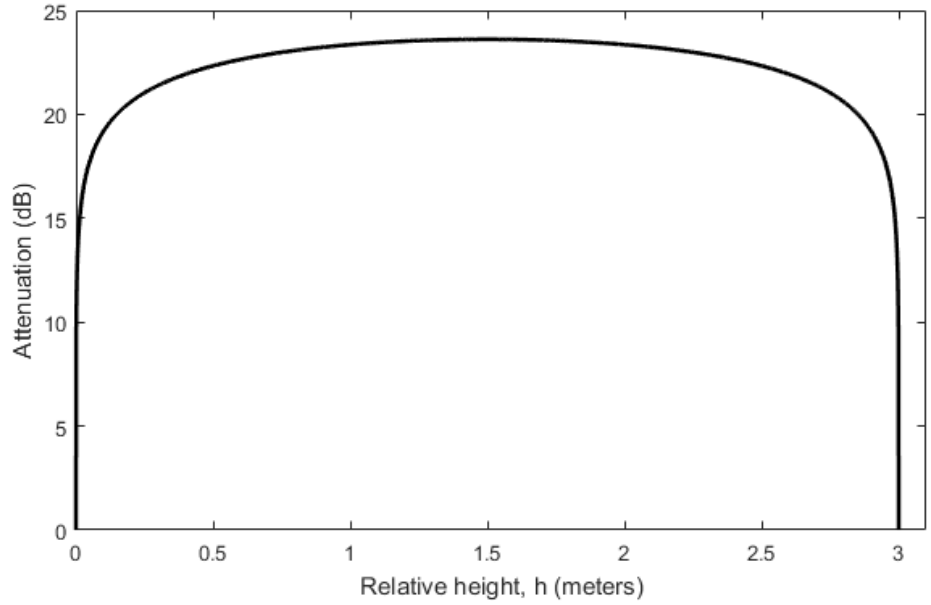

Figure 4.14: Through vegetation attenuation versus relative height at 37 GHz considering a spherical crown

Figure 4.13 shows the relationship between relative height and vegetation depth for a crown modelled as a sphere at 37 GHz. For a spherical crown, the vegetation depth increases as the relative height increases up till 1.5 m. For relative height higher than 1.5 m, the vegetation depth decreases as relative height increases.

Figure 4.14 shows the relationship between through vegetation attenuation and relative height for a spherical crown at 37 GHz using London Plane's parameters at 37 GHz. Signal attenuation increases with a very steep slope from 0 dB to around 20 dB as relative height ranges from 0 to 0.2 m. The signal attenuation decreases with a steep slope from around 20 dB to 0 dB as relative height increases from 2.8 m to 3 m. The attenuation is zero when relative height is 0 m and 3 m. This is because the vegetation depth is zero when relative height is 0 m and 3 m. In other words, the signal passes by the surface of crown and not passing through it. As a result, scattering and absorption of the signal by the vegetative medium does not happen. This results in zero attenuation by the vegetation. Based on Figure 4.13 and Figure 4.14, it is clear that through vegetation attenuation is proportional to vegetation depth for a spherical crown.

4.9 Comparison between Enhanced Model and Original Model

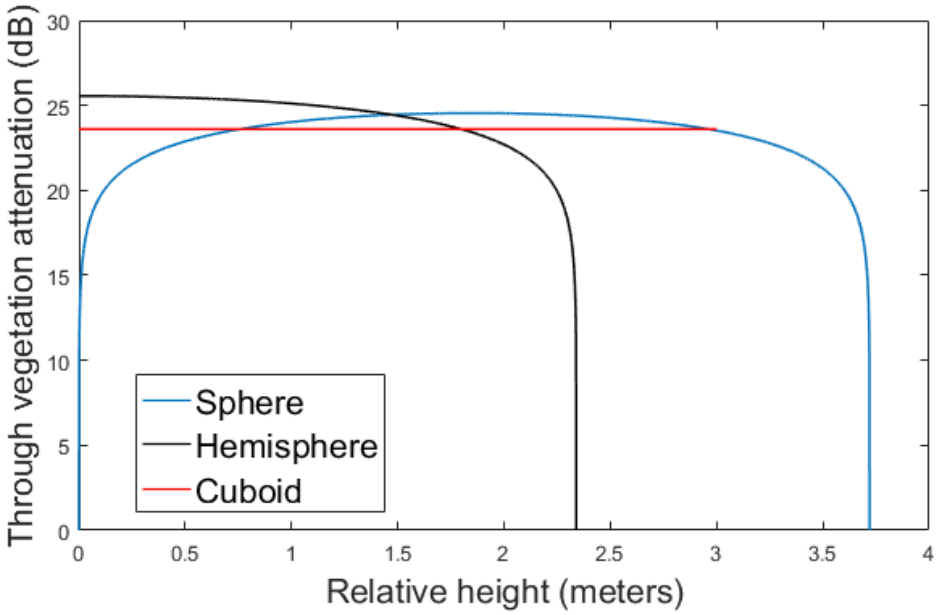

Figure 4.15: Comparison between enhanced model (using hemispherical and spherical crown) and original model (cuboid crown)

Figure 4.15 shows three plots of through vegetation attenuation (dB) against relative height (meters) at 37 GHz with the volume of vegetation fixed at 27 m^3. They are plots for hemispherical, spherical and cuboid crown respectively. The through vegetation attenuation for cuboid or the original through vegetation component of the ITU-R model remains at 23.61 dB as relative height increases. For hemispherical crown, the through vegetation attenuation peaks at 25.55 dB. The peak attenuation for hemispherical crown is 7.59 % different from the constant signal attenuation for a cuboid crown. For spherical crown, the through vegetation attenuation peaks at 24.55 dB. The peak attenuation for spherical crown is 3.83 % different from the constant signal attenuation for a cuboid crown. Based on comparison, it is evident that signal attenuation varies for different crown shapes even though the vegetative volume is the same. On the other hand, the signal attenuation varies in different trends as relative height increases as shown in Figure 4.15.

CHAPTER 5 CONCLUSIONS

5.1 Summary and Conclusions

In this project, investigation into background processes of mm-wave propagation with presence of vegetation such as through vegetation scattering and absorption, ground reflection and diffraction were conducted.

Firstly, attenuation due to through vegetation component at 37 GHz and 61.5 GHz was investigated. It was found that the curves of through vegetation attenuation and vegetation depth have dual slope characteristic. In addition, through vegetation attenuation is relatively higher at a higher frequency.

The attenuation due to ground reflection increases as grazing angle increases for horizontal polarization. For a D2D connection, it is safe to guess that the grazing angle is around 45 º if the users are standing. Ground reflection loss for horizontal polarization is around 10 to 20 dB for all types of ground surface at 45 º. As for vertical polarization, the curves of attenuation due to ground reflection against grazing angle have a "camel hump" shape, which has higher ground reflection loss at 45º. In addition, for most of the cases, the attenuation is higher as the water content of the ground on which the signal is reflected off is higher.

It was found that top diffraction loss decreases as the transmitter or receiver are farther away from the points of diffraction. The top diffraction loss increases as the width of vegetative medium increases. As for side diffractions, the loss is minimal when the link is located near the edge of the tree. In addition, the side diffracted loss increases as the width of the tree increases.

The enhancement to the through vegetation component of ITU-R model or the RET model was done by modelling the crown of tree as sphere and hemisphere based on crown shape of tree species popular for tree planting in Kuala Lumpur, Malaysia. The through vegetation attenuation increases when the depth of vegetation increases. For a tree with a hemispherical crown, the vegetation depth decreases as the relative height increases. Through vegetation attenuation decreases when relative height

increases. For a tree with spherical crown, the through vegetation attenuation increases initially, levels off and eventually decreases as the relative height increases. The peak attenuations for hemispherical and spherical crown are 7.59 % and 3.83 % different from the constant signal attenuation for a cuboid crown respectively. The proposed enhanced model for predicting through vegetation attenuation for trees with crown shapes such as hemisphere and sphere provide more realistic and accurate approximations to urban trees in Kuala Lumpur, Malaysia.

Overall, it was discovered that the loss of diffractions are in orders of hundreds of dB. The through vegetation attenuation and ground reflection loss are in orders of tens of dB. In conclusion, the main contributor of the received signal when facing a blocking vegetative medium is the through vegetation component or the direct path component, which was investigated using RET model. For a D2D connection, ground reflected signal contribute to the received signal. On the other hand, the diffracted signals are negligible contributor to the received signal as the losses are over 100 dB. The findings of this project are useful for future 5G deployment in Malaysia if 37 to 40.5 GHz band is selected as a 5G band.

5.2 Areas of Future Research

One of the limitations of current model is the lack of parameters for RET model at other frequencies of mm-wave spectrum and tree species other than London Plane. The parameters for other frequencies and species can be obtained through measurement. Secondly, the current model only investigates the effects of vegetative medium on a single frequency. Investigation of effects of vegetative medium on mm-wave propagation over an entire band will be a more comprehensive study which can be referenced for future 5G deployment.

REFERENCES

[1] Jeffrey G. Andrews et al., "What Will 5G Be?," *IEEE Journal on Selected Areas in Communications*, vol. 32, no. 6, pp. 1065 - 1082, 2014.

[2] International Telecommunication Union, *IMT Vision - "Framework and overall objectives of the future development of IMT for 2020 and beyond"*, Recommendation ITU-R M.2083, 2015.

[3] S. Sun, R. Mayzus, H.Zhao, Y. Azar, K. Wang, G.N. Wong, J.K. Schulz, M. Samimi and F. Gutierrez T. S. Rappaport, "Millimeter Wave Mobile Communications for 5G Cellular: It Will Work!," *IEEE Access*, pp. 335-349, May 2013.

[4] International Telecommunication Union, Resolution 238 (WRC-15), 2015.

[5] METIS, *Deliverable D1.4: METIS Channel Models*, 2015.

[6] National Instruments. (2016, June). mmWave: The Battle of the Bands. [Online]. Available: http://www.ni.com/white-paper/53096/en/.

[7] International Telecommunication Union, *Radio Regulations Articles*, 2012.

[8] Malaysian Communications and Multimedia Commission 2014, *Spectrum Plan*, 2014.

[9] Office of Communications. (2015, January). Spectrum above 6 GHz for future mobile communications. [Online]. Available: https://www.ofcom.org.uk/__data/assets/pdf_file/0023/69422/spectrum_above_6_ghz_cfi.pdf.

[10] Y.S.Meng and Y. H. Lee, "Investigations of Foliage Effect on Modern Wireless Communication Systems : A Review," *Progress in Electromagnetics Research*, vol. 105, pp. 313-332, 2010.

[11] David Ndzi, Andrew Seville, Enric Vilar, John Austin Nick Savage, "Radio wave propagation through vegetation: Factors influencing signal attenuation,"

Radio Science, vol. 38, no. 5, October 2003.

[12] A Seville, J Richter, D Ndzi, N Savage, RFS Caldeirinha,AK Shukla, MO Al-Nuaimi, K Craig, E Vilar and J Austin NC Rogers, "A Generic Model of 1-60 GHz," QinetiQ, 2002.

[13] R.A. Johnson and F. Schwering, "A Transport Theory of Millimeter Wave Propagation in Woods and Forests," US Army Communications - Electronics Command, Fort Monmouth, New Jersey, Technical Report February 1985.

[14] Y. H. Lee, and B. C. Ng Y. S. Meng, "Study of Propagation Loss Prediction in Forest Environment," *Progress In Electromagnetics Research* , vol. 17, pp. 117-133, 2009.

[15] International Telecommunication Union, *Attenuation in Vegetation*, Recommendation ITU-R P.833-4, 2003.

[16] Gabor Fodor. (2014, July). D2D Communications-What Part Will It Play in 5G?. [Online]. Available: https://www.ericsson.com/research-blog/5g/device-device-communications/.

[17] International Telecommunication Union, *Attenuation in Vegetation*, Recommendation ITU-R P.833-8, 2013.

[18] International Telecommunication Union, *Reflections from the surface of the earth*, CCIR Report. 1008-1, 1990.

[19] International Telecommunication Union, E*lectrical Characteristics of the Surface of the Earth*, Recommendation ITU-R P.527-3:, 1992.

[20] International Telecommunication Union, *Propagation by diffraction*, Recommendation ITU-R P.526-13:, 2013.

[21] Bassem R. Mahafza, *Radar Signal Analysis and Processing Using MATLAB*. Alabama, U.S.A: CRC Press, 2008.

[22] E. Philip, M. Adnan and M. Siti Zakiah M. Sreetheran, "A historical perspective of urban tree planting ," Food and Agriculture Organization of the United Nations.

[23] International Telecommunication Union, *Propagation data and prediction methods for the planning of indoor radiocommunication systems and radio local area networks in the frequency range 300 MHz to 100 GHz*, Recommendation ITU-R P.1238-8, 2015.

APPENDIX A: MATLAB Codes for Empirical Models

medmodels.m

```
F=20;
f=20000;
w = @(d) [(0.45*(F.^0.284)*d).*(0 <= d & d<14) + ...
    (1.33*(F.^0.284)*(d.^0.588)).*(d>=14 & d<400)];
d=linspace(0,25);
costInleaf = 15.6*(f.^-0.009)*(d.^0.26);
costOutleaf = 26.6*(f.^-0.2)*(d.^0.5);
fiturInleaf = 0.39*(f.^0.39)*(d.^0.25);
fiturOutleaf = 0.37*(f.^0.18)*(d.^0.59);
figure
plot(d,w(d),d,costInleaf,d,fiturInleaf,d,costOutleaf,d,fiturOutleaf)
;
title('Vegetation attenuation at 20GHz')
xlabel('vegetation depth(meters)')
ylabel('Attenuation(dB)')
legend('Weissberger','COST 235 In-leaf','FITUR In-leaf',...
'COST 235 Out-of-leaf','FITUR Out-of-leaf')
```

maModel.m

```
d=0:1000;
%2117MHz
%mixed coniferous-deciduous
%vegetation (mixed forest) near St. Petersburg (Russia)
sa=0.34;
Am=34.1;
MA=Am*(1-exp(-d*sa/Am));
figure
plot(d,MA)
title('Vegetation attenuation at 2.117 GHz')
xlabel('vegetation depth(meters)')
ylabel('Attenuation(dB)')
```

nzgmodel.m

```
%nzg
d=0:100;
a=0.2;b=1.27;c=0.63;ko=6.57;Rf=0.0002;Ao=10;
f=20;
Ro=a*f;
Rinf=b/(f.^c);
Amin = 2;
k=ko - 10*log10(Ao*(1-exp(-Amin/Ao))*(1-exp(-Rf*f)));

Ain=Rinf*d + k*(1-exp(-(Ro-Rinf)/k*d));
a=0.16;b=2.59;c=0.85;ko=12.6;Rf=2.1;Ao=10;
f=20;
Ro=a*f;
Rinf=b/(f.^c);
Amin = 2;
k=ko - 10*log10(Ao*(1-exp(-Amin/Ao))*(1-exp(-Rf*f)));
Aout=Rinf*d + k*(1-exp(-(Ro-Rinf)/k*d));

a=0.2;b=1.27;c=0.63;ko=6.57;Rf=0.0002;Ao=10;
f=40;
Ro=a*f;
Rinf=b/(f.^c);
```

```
Amin = 2;
k=ko - 10*log10(Ao*(1-exp(-Amin/Ao))*(1-exp(-Rf*f)));

Ain40=Rinf*d + k*(1-exp(-(Ro-Rinf)/k*d));
a=0.16;b=2.59;c=0.85;ko=12.6;Rf=2.1;Ao=10;
f=40;
Ro=a*f;
Rinf=b/(f.^c);
Amin = 2;
k=ko - 10*log10(Ao*(1-exp(-Amin/Ao))*(1-exp(-Rf*f)));
Aout40=Rinf*d + k*(1-exp(-(Ro-Rinf)/k*d));

plot(d,Ain,d,Aout,d,Ain40,d,Aout40);
title('Vegetation attenuation')
xlabel('vegetation depth(meters)')
ylabel('Attenuation(dB)')
legend('NZG in-leaf 20GHZ','NZG Out-of-leaf 20GHZ','NZG in-leaf
40GHZ','NZG Out-of-leaf 40GHZ')
```

APPENDIX B: MATLAB Codes for ITU-R Model

amplitudeFactors.m

```
function y = amplitudeFactors(s)
n = 6:11;
mu_n = -cos(n*pi/11);
B = [0 0 0 0 0 1/(sin(pi/22)^2)];
B = B';
A= zeros(6,6);
for i = 1:6
    A(i,:) = 1./(1-mu_n(i)./s);
end
y = linsolve(A,B);
end
```

attenuationCoefficients.m

```
function S = attenuationCoefficients( a ,W )

Pn = zeros(12,1);
mu_n = zeros(12,1);
s = zeros(12,1);
Wbar = (1 - a)*W/(1-a*W);

for i = 1:12
    if i == 1 || i == 12
        Pn(i) = (sin(pi/(2*11)))^2;
        mu_n(i) = -cos((i-1)*pi/11);
    else
        Pn(i) = sin(pi/11)*sin((i-1)*pi/11);
        mu_n(i) = -cos((i-1)*pi/11);
    end
end

syms s
temp = Pn./(1-mu_n/s);
CE = Wbar/2*sum(temp(:));
S =solve(CE == 1,s);
S = vpa(S);
S = sort(S);
```

ret.m

```
clear all;
close all;
clc;
freq = input('frequency =>');

if freq == 37
    %37GHz London Plane input parameters
    a=0.95;
    w= 0.95;
    Beta = 18;
    sigmaT=0.441;


elseif freq == 61.5
    %61.5GHz London Plane input parameters
```

```
    a=0.25;
    w=0.50;
    Beta = 2 ;
    sigmaT=0.498;
end

S = attenuationCoefficients(a,w);
s = S(7:12);
s = s';
Ak = amplitudeFactors(s);
Ak = Ak';

crown = input('Crown type =>');
if strcmp(crown,'cuboid')==1
    d = 0:3;
elseif strcmp(crown,'sphere')==1
    h = 0:0.001:3;
    r = sqrt(((1.5).^2) - ((h - 1.5).^2));
    d = r.*2;
elseif strcmp(crown,'halfsphere')==1
    h = 0:0.001:1.5;
    r = sqrt(((1.5).^2) - (h.^2));
    d = r.*2;
end

% initialize vars
beamWidth = 10;
m = 1:10;
tau = sigmaT * d;
taubar = (1 - a*w) * tau;
delta = 0.6*beamWidth;
betaS = 0.6*Beta;
qm = 4./(delta^2 + m*betaS^2);

% term 1
term1 = exp(-tau);

% term 2
qM = qm(10);
term2part1 = (exp(-taubar) - exp(-tau))*qM;

fac = factorial(m);
temp = zeros(length(tau),10);
for i = 1:length(tau)
    temp(i,:) = (1./fac.*(a*w*tau(i)).^m).*(qm - qM);
end
temp = temp';
term2part2 = exp(-tau).*sum(temp);

term2 = (delta^2)/4*(term2part1 + term2part2);

% term 3

term3part1 = -exp(-taubar)*1/sin(pi/22)^2;

temp2 = zeros(length(taubar),6);
mu_N = -cos(pi);
```

```
for i = 1:length(taubar)
    temp2(i,:) = (Ak.*exp(taubar(i)./s))./(1-mu_N./s);
end

temp2 = temp2';

term3part2 = sum(temp2);
term3 = (delta^2)/2*(term3part1 + term3part2);

%Lscat
L = 10*log10(term1 + term2 + term3);

if strcmp(crown,'cuboid')==1
    plot(d,L)
elseif strcmp(crown,'sphere')==1 || strcmp(crown,'halfsphere')==1
    plot(h,L);
end
```

groundReflection.m

```
clear all;
close all;
clear all;
%Calculate reflection coefficient
%relative permittivity and conductivity
%Uncomment relPerm and cond for condition of ground
%u want to use

%dry ground
% relPerm = 5;
% cond = 10;

%medium dry ground
% relPerm = 5;
% cond = 8;

%  wet ground
relPerm = 3;
cond = 0.45;

freq = 37e9;
lambda = physconst('LightSpeed')/freq;
psi = 0.01:0.05:90;
angle = psi.*pi./180;
%calculate complex permittivity
complexPerm = relPerm - 1i*60*lambda*cond;

% for horizontal polarization
Ch = complexPerm - (cos(angle)).^2;
%for vertical polarization
Cv = (complexPerm - (cos(angle)).^2)./((complexPerm).^2);

RoVer = (sin(angle) - sqrt(Cv))./(sin(angle) + sqrt(Cv));
RoHor = (sin(angle) - sqrt(Ch))./(sin(angle) + sqrt(Ch));

brewsterAngle = radtodeg(asin(1/sqrt(abs(complexPerm))));
```

```
figure(1)
plot(psi,abs(RoVer),psi,abs(RoHor));
d0 = 103;
d1 = sin(angle).*103./sin(pi-2.*angle);
d2 = d1;
Lgroundver = 20*log((d1+d2)/d0)-20*log(abs(RoVer));
Lgroundhor = 20*log((d1+d2)/d0)-20*log(abs(RoHor));
figure(2)
plot(psi,Lgroundver)
figure(3)
plot(psi,Lgroundhor)
```

DoubleIsolatedDiffractionClass.m

```
classdef DoubleIsolatedDiffractionClass
    properties
        a;
        b;
        c;
        halft;
        lambda;

    end
    methods
        function L = calculateLoss(obj)
            h1 = obj.halft - obj.halft*obj.a/(obj.a+obj.b);
            h2 = obj.halft - obj.halft*obj.c/(obj.c+obj.b);
            d2 = obj.b;
            d1 = norm([obj.a,obj.halft]);
            d3 = norm([obj.c,obj.halft]);
            v1 = h1*sqrt(2/obj.lambda*(1/d1+1/d2));
            v2 = h2*sqrt(2/obj.lambda*(1/d2+1/d3));

            C = @(s) cos((pi*(s.^2))/2);
            S = @(s) sin((pi*(s.^2))/2);

            Cv1 = integral(C,0,v1);
            Sv1= integral(S,0,v1);
            Cv2 = integral(C,0,v2);
            Sv2= integral(S,0,v2);
            % Jv is loss
            Jv1 = -20.*log(sqrt((1-Cv1-Sv1).^2 + (Cv1-Sv1).^2)/2);
            Jv2 = -20.*log(sqrt((1-Cv2-Sv2).^2 + (Cv2-Sv2).^2)/2);
            Lc =
10.*log((obj.a+obj.b)*(obj.b+obj.c)/(obj.b*(obj.a+obj.b+obj.c)));

            L = Jv1 + Jv2 + Lc;
        end
    end
end
```

doubleisolatedDiffraction.m

```
%Double isolated diffraction
clear all;
close all;
clc
% signal's freq and wavelength
```

```
freq = 37e9;
lambda = physconst('LightSpeed')/freq;

% top diffracted
%t - height of tree, d- depth of tree

halft = 3;
param = input('parameter under investigation for top diffraction
=>');

if strcmp(param,'a')==1
    b = 3;
    c = 10;
    Ltop_study = zeros(100,1);
    for x = 10:100
        topDiffracted = DoubleIsolatedDiffractionClass;
        topDiffracted.halft = halft;
        topDiffracted.a = x;
        topDiffracted.b = b;
        topDiffracted.c = c;
        topDiffracted.lambda = lambda;
        Ltop = calculateLoss(topDiffracted);
        Ltop_study(x) = Ltop;
    end
    parameter = 10:100;
    plot(parameter,Ltop_study(10:100));
elseif strcmp(param,'b')==1
    a = 10;
    c = 10;
    Ltop_study = zeros(5,1);
    for x = 1:5
        topDiffracted = DoubleIsolatedDiffractionClass;
        topDiffracted.halft = halft;
        topDiffracted.a = a;
        topDiffracted.b = x;
        topDiffracted.c = c;
        topDiffracted.lambda = lambda;
        Ltop = calculateLoss(topDiffracted);
        Ltop_study(x) = Ltop;
    end
    parameter = 1:5;
    plot(parameter,Ltop_study);
elseif strcmp(param,'c')==1
    b = 3;
    a = 10;
    Ltop_study = zeros(100,1);
    for x = 10:100
        topDiffracted = DoubleIsolatedDiffractionClass;
        topDiffracted.halft = halft;
        topDiffracted.a = a;
        topDiffracted.b = b;
        topDiffracted.c = x;
        topDiffracted.lambda = lambda;
        Ltop = calculateLoss(topDiffracted);
        Ltop_study(x) = Ltop;
    end
    parameter = 10:100;
    plot(parameter,Ltop_study(10:100));
```

```
end
%side diffracted

sideparam = input('parameter under investigation for side
diffraction=>');
if strcmp(sideparam,'p')==1
    a = 10;
    b = 3;
    c = 10;
    w = 3;
    sideloss = ones(11,1);

    count = 0;
    for p = 0:0.1:1
        count = count + 1;
        percentWidth_a = p;
        %side A diffracted
        halft_a = percentWidth_a.*w;
        side_a_Diffracted = DoubleIsolatedDiffractionClass;
        side_a_Diffracted.halft = halft_a;
        side_a_Diffracted.a = a;
        side_a_Diffracted.b = b;
        side_a_Diffracted.c = c;
        side_a_Diffracted.lambda = lambda;
        Lside_a = calculateLoss(side_a_Diffracted);

        %side b diffracted
        halft_b = (1-percentWidth_a).*w;
        side_b_Diffracted = DoubleIsolatedDiffractionClass;
        side_b_Diffracted.halft = halft_b;
        side_b_Diffracted.a = a;
        side_b_Diffracted.b = b;
        side_b_Diffracted.c = c;
        side_b_Diffracted.lambda = lambda;
        Lside_b = calculateLoss(side_b_Diffracted);
        sideloss(count) = Lside_a+Lside_b;
    end
    p = 0:0.1:1;
    plot(p,sideloss)

elseif strcmp(sideparam,'w')==1
    a = 10;
    b = 3;
    c = 10;
    sideloss = ones(5,1);
    p = 0.5;
    count = 0;
    for w = 1:5
        count = count + 1;
        percentWidth_a = p;
        %side A diffracted
        halft_a = percentWidth_a.*w;
        side_a_Diffracted = DoubleIsolatedDiffractionClass;
        side_a_Diffracted.halft = halft_a;
        side_a_Diffracted.a = a;
        side_a_Diffracted.b = b;
        side_a_Diffracted.c = c;
        side_a_Diffracted.lambda = lambda;
```

```
        Lside_a = calculateLoss(side_a_Diffracted);

        %side b diffracted
        halft_b = (1-percentWidth_a).*w;
        side_b_Diffracted = DoubleIsolatedDiffractionClass;
        side_b_Diffracted.halft = halft_b;
        side_b_Diffracted.a = a;
        side_b_Diffracted.b = b;
        side_b_Diffracted.c = c;
        side_b_Diffracted.lambda = lambda;
        Lside_b = calculateLoss(side_b_Diffracted);
        sideloss(count) = Lside_a+Lside_b;
    end
    w = 1:5;
    plot(w,sideloss)
end
```

retCompare.m

```
clear all;
close all;
clc;
freq = input('frequency =>');

if freq == 37
    %37GHz London Plane input parameters
    a=0.95;
    w= 0.95;
    Beta = 18;
    sigmaT=0.441;


elseif freq == 61.5
    %61.5GHz London Plane input parameters
    a=0.25;
    w=0.50;
    Beta = 2 ;
    sigmaT=0.498;
end

S = attenuationCoefficients(a,w);
s = S(7:12);
s = s';
Ak = amplitudeFactors(s);
Ak = Ak';

crown = input('Crown type =>');
if strcmp(crown,'cuboid')==1
    h = 0:0.001:3;
    d = ones(1,length(h))*3;
elseif strcmp(crown,'sphere')==1
    h = 0:0.001:3.72;
    r = sqrt(((1.86).^2) - ((h - 1.86).^2));
    d = r.*2;
elseif strcmp(crown,'halfsphere')==1
    h = 0:0.001:2.34;
    r = sqrt(((2.34).^2) - (h.^2));
    d = r.*2;
```

```
end

% initialize vars
beamWidth = 10;
m = 1:10;
tau = sigmaT * d;
taubar = (1 - a*w) * tau;
delta = 0.6*beamWidth;
betaS = 0.6*Beta;
qm = 4./(delta^2 + m*betaS^2);

% term 1
term1 = exp(-tau);

% term 2
qM = qm(10);
term2part1 = (exp(-taubar) - exp(-tau))*qM;

fac = factorial(m);
temp = zeros(length(tau),10);
for i = 1:length(tau)
    temp(i,:) = (1./fac.*(a*w*tau(i)).^m).*(qm - qM);
end
temp = temp';
term2part2 = exp(-tau).*sum(temp);

term2 = (delta^2)/4*(term2part1 + term2part2);

% term 3

term3part1 = -exp(-taubar)*1/sin(pi/22)^2;

temp2 = zeros(length(taubar),6);
mu_N = -cos(pi);
for i = 1:length(taubar)
    temp2(i,:) = (Ak.*exp(taubar(i)./s))./(1-mu_N./s);
end

temp2 = temp2';

term3part2 = sum(temp2);
term3 = (delta^2)/2*(term3part1 + term3part2);

%Lscat
L = 10*log10(term1 + term2 + term3);

if strcmp(crown,'cuboid')==1
    plot(h,L)
elseif strcmp(crown,'sphere')==1 || strcmp(crown,'halfsphere')==1
    plot(h,L);
end
```